ECSS-E-HB-20-06A
15 May 2019

Space engineering

Assessment of space worst case charging handbook

ECSS Secretariat
ESA-ESTEC
Requirements & Standards Division
Noordwijk, The Netherlands

Foreword

This Handbook is one document of the series of ECSS Documents intended to be used as supporting material for ECSS Standards in space projects and applications. ECSS is a cooperative effort of the European Space Agency, national space agencies and European industry associations for the purpose of developing and maintaining common standards.

The material in this Handbook is defined in terms of description and recommendation how to organize and perform the work of making an assessment of worst case charging on a spacecraft.

This handbook has been prepared by the ECSS-E-HB-20-06A Working Group, reviewed by the ECSS Executive Secretariat and approved by the ECSS Technical Authority.

Disclaimer

Published by: ESA Requirements and Standards Division
ESTEC, P.O. Box 299,
2200 AG Noordwijk
The Netherlands

Change log

ECSS-E-HB-20-06A 15 May 2019	First issue

Table of contents

Figures

Tables

Introduction

Spacecraft charging occurs due to the deposition of charge on spacecraft surfaces or in internal materials due to charged particles from the environment. Resulting high voltages and high electric fields cause electrostatic discharges which are a hazard to many spacecraft systems. Broadly speaking, spacecraft charging can be divided into surface charging, which is caused by plasma particles with energy up to several 10s of keV and internal charging which is caused by trapped radiation electrons with energy around 0,2 MeV and above.

Both surface and internal charging have been associated with malfunctions and damage to spacecraft systems over many years.

1
Scope

Common engineering practices involve the assessment, through computer simulation (with software like NASCAP [RD.4] or SPIS [RD.5]), of the levels of absolute and differential potentials reached by space systems in flight. This is usually made mandatory by customers and by standards for the orbits most at risk such as GEO or MEO and long transfers to GEO by, for example, electric propulsion.

The ECSS-E-ST-20-06 standard requires the assessment of spacecraft charging but it is not appropriate in a standard to explain how such an assessment is performed. It is the role of this document ECSS-E-HB-20-06, to explain in more detail important aspects of the charging process and to give guidance on how to carry out charging assessment by computer simulation.

The ECSS-E-ST-10-04 standard specifies many aspects of the space environment, including the plasma and radiation characteristics corresponding to worst cases for surface and internal charging. In this document the use of these environment descriptions in worst case simulations is described.

The emphasis in this document is on high level charging in natural environments. One aspect that is currently not addressed is the use of active sources e.g. for electric propulsion or spacecraft potential control. The tools to address this are still being developed and this area can be addressed in a later edition.

2 References

[RD.1]	ECSS-S-ST-00-01, ECSS system – Glossary of terms
[RD.2]	ECSS-E-ST-10-04, Space engineering, Space environment
[RD.3]	ECSS-E-ST-20-06, Space engineering, Spacecraft charging
[RD.4]	Myron J. Mandell, Victoria A. Davis, David L. Cooke, Member, IEEE, Adrian T. Wheelock, and C. J. Roth, Nascap-2k Spacecraft Charging Code Overview, IEEE TRANSACTIONS ON PLASMA SCIENCE, VOL. 34, NO. 5, OCTOBER 2006
[RD.5]	Benoit Thiébault, Benjamin Jeanty-Ruard, Pierre Souquet, Julien Forest, Jean-Charles Matéo-Vélez, Pierre Sarrailh, David Rodgers, Alain Hilgers, Fabrice Cipriani, Denis Payan, and Nicolas Balcon, SPIS 5.1: An Innovative Approach for Spacecraft Plasma Modeling, IEEE TRANSACTIONS ON PLASMA SCIENCE, VOL. 43, NO. 9, SEPTEMBER 2015. [SPIS can be downloaded from http://dev.spis.org/projects/spine/home/spis]
[RD.6]	D. Payan, V. Inguimbert, and J.-M. Siguier, ESD and secondary arcing powered by the solar array – toward full arc free power lines, 14th SCTC, ESTEC, 2016
[RD.7]	M. Bodeau, Updated current and voltage thresholds for sustained arcs in power systems, IEEE Trans. on Plasma Science, Vol. 42, No. 7, 2014
[RD.8]	C. Imhof, H. Mank, and J. Lange, Charging simulations for a low earth orbit satellite with SPIS using different environmental inputs, 14th SCTC, ESTEC, 2016
[RD.9]	Yeh and Gussenhoven, The statistical electron environment for Defense Meteorological Satellite Program eclipse charging, JGR, vo.92, no.A7, pp.7705-7715, 1987
[RD.10]	F. Lei, P. R. Truscott, C. S. Dyer, B. Quaghebeur, D. Heynderickx, P. Nieminen, H. Evans, and E. Daly, MULASSIS: A Geant4-Based Multilayered Shielding Simulation Tool, IEEE TRANSACTIONS ON NUCLEAR SCIENCE, VOL. 49, NO. 6, DECEMBER 2002
[RD.11]	Adamec, V. and J. Calderwood, J Phys. D: Appl. Phys., 8, 551-560, 1975.
[RD.12]	D.J.Rodgers, K. Ryden G.L. Wrenn, P.M. Latham, J. Sorensen, & L. Levy (1998). An Engineering Tool for the Prediction of Internal Dielectric Charging, Proc. 6th Spacecraft Charging Technology Conference, Hanscom, USA
[RD.13]	R. Hanna, T. Paulmier, P. Molinie, M. Belhaj, B. Dirassen, D. Payan and N. Balcon, J. Appl. Phys. 115, 033713 (2014)]
[RD.14]	Insoo Jun, Henry B. Garrett, Wousik Kim, and Joseph I. Minow, Review of an Internal Charging Code, NUMIT, IEEE TRANSACTIONS ON PLASMA SCIENCE, VOL. 36, NO. 5, OCTOBER 2008

[RD.15]	F. Lei, D. Rodgers and P. Truscott, MCICT MONTE-CARLO INTERNAL CHARGING TOOL, Proc. 14th Spacecraft Charging Technology Conference, ESA/ESTEC, Noordwijk, NL, 08 APRIL 2016
[RD.16]	Alex Hands, Keith Ryden, Craig Underwood, David Rodgers and Hugh Evans, A New Model of Outer Belt Electrons for Dielectric Internal Charging (MOBE-DIC) IEEE TRANSACTIONS ON NUCLEAR SCIENCE, VOL. 62, NO. 6, DECEMBER 2015
[RD.17]	G. P. Ginet, P. O'Brien, S. L. HustonW. R. Johnston, T. B. Guild, R. Friedel, C. D. Lindstrom, C. J. Roth, P. Whelan, R. A. Quinn, D. Madden, S. Morley, Yi-Jiun Su, AE9, AP9 and SPM: New Models for Specifying the Trapped Energetic Particle and Space Plasma Environment, Space Science Reviews November 2013, Volume 179, Issue 1–4, pp 579–615
[RD.18]	B. Jeanty-Ruard, A. Trouche, P. Sarrailh, J. Forest. Advanced CAD tool and experimental integration of GRAS/GEANT-4 for internal charging analysis in SPIS. Spacecraft Charging Technology Conference SCTC 2016, Apr 2016, NOORDWIJK, Netherlands.
[RD.19]	D. Payan, A. Sicard-Piet, J.C. Mateo-Velez, D.Lazaro, S. Bourdarie, et al.. Worst case of Geostationary charging environment spectrum based on LANL flight data. Spacecraft Charging Technology Conference 2014 (13th SCTC), Jun 2014, PASADENA, United States.
[RD.20]	Gussenhoven, M.S. and E. G. Mullen (1983), Geosynchronous environment for severe spacecraft charging, J. Spacecraft and Rockets 20, N°1, p. 26.
[RD.21]	Matéo-Vélez, J.-C., Sicard, A., Payan, D., Ganushkina, N., Meredith, N. P., & Sillanpäa, I. (2018). Spacecraft surface charging induced by severe environments at geosynchronous orbit. Space Weather, 16.
[RD.22]	NASA-HDBK-4002A, Mitigating in space charging effects – a guideline, 03-03-2011
[RD.23]	Inguimbert, V., Siguier, J. M., Sarrailh, P., Matéo-Vélez, J. C., Payan, D., Murat, G., & Baur, C. Influence of Different Parameters on Flashover Propagation on a Solar Panel. IEEE Transactions on Plasma Science (2017)
[RD.24]	E. Amorim, D. Payan, R. Reulet, and D. Sarrail, "Electrostatic discharges on a 1 m2 solar array coupon—Influence of the energy stored on coverglass on flashover current," in Proc. 9th Spacecraft Charging Technol. Conf., Tsukuba, Japan, Apr. 2005
[RD.25]	R. Briet,, "Scaling laws for pulse waveforms from surface discharges," in Proc. 9th SCTC, Tsukuba, Japan, Apr. 2005.,
[RD.26]	D. C. Ferguson and B. V. Vayner, "Flashover current pulse formation and the perimeter theory," IEEE Trans. Plasma Sci., vol. 41, no. 12, pp. 3393–3401, Dec. 2013
[RD.27]	J.-F. Roussel et al., "SPIS multiscale and Multiphysics capabilities: Development and application to GEO charging and flashover modelling," IEEE Trans. Plasma Sci., vol. 40, no. 2, pp. 183–191, Feb. 2012.
[RD.28]	J. A. Young and M. W. Crofton, "The effects of material at arc site on ESD propagation," in Proc. 14th SCTC, Noordwijk, The Netherlands, Apr., pp. 1–7, 2016
[RD.29]	P. Sarrailh et al., "Plasma bubble expansion model of the flash-over current collection on a solar array-comparison to EMAGS3 results," IEEE Trans. Plasma Sci., vol. 41, no. 12, pp. 3429–3437, Dec. 2013
[RD.30]	V. Inguimbert et al., "Measurements of the flashover expansion on a real-solar panel—Preliminary results of EMAGS3 project," IEEE Trans. Plasma Sci., vol. 41, no. 12, pp. 3370–3379, Dec. 2013.

[RD.31]	A. Gerhard et al., "Analysis of solar array performance degradation during simulated flashover discharge experiments on a full panel and using a simulator circuit," IEEE Trans. Plasma Sci., vol. 43, no. 11, pp. 3933–3938, Nov. 2015
[RD.32]	Sarno-Smith, Lois K., Larsen, Brian A., Skoug, Ruth M., Liemohn, Michael W., Breneman, Aaron, Wygant, John R., Thomsen, Michelle F., Spacecraft surface charging within geosynchronous orbit observed by the Van Allen Probes, Space Weather, Volume 14, Issue 2, Pages 151–164, February 2016
[RD.33]	Ganushkina, N. Yu., Amariutei, O. A., Welling, D., Heynderickx, D., Nowcast model for low-energy electrons in the inner magnetosphere, Space Weather, Volume 13, issue 1, pp. 16-34, 2015
[RD.34]	NASA Technical paper 2361,1984 Design guidelines for assessing and controlling spacecraft charging effects
[RD.35]	Matéo-Vélez, J.-C., Sicard, A., Payan, D., Ganushkina, N., Meredith, N. P., & Sillanpäa, I. (2018). Spacecraft surface charging induced by severe environments at geosynchronous orbit. Space Weather, 16. https://doi.org/10.1002/2017SW001689

3
Terms, definitions and abbreviated terms

3.1 Terms from other documents

a. For the purpose of this document, the terms and definitions from ECSS-S-ST-00-01 apply, in particular the following terms:

1. environment

3.2 Abbreviated terms

For the purpose of this document, the abbreviated terms from ECSS-S-ST-00-01 apply and in particular the following:

Abbreviation	Meaning
AU	astronomical unit
BOL	beginning-of-life
CAD	computer-aided design
CSDA	continuous slowing down approximation (relating to range of radiation in matter)
EMC	electromagnetic compatibility
ESD	electrostatic discharge
EOL	end-of-life
GDML	Geometry Definition Markup Language
GUI	graphical user interface
GEO	geostationary orbit
GTO	geostationary transfer orbit
MEO	medium Earth orbit
MLI	multi-layer insulation
LANL	LoaSAlamos National Laboratory
LEO	low Earth orbit
SEE	secondary electron emission

In addition the following acronyms are used in this document

Acronym	Meaning
AE9/SPM	United States Airforce electron environment model / Standard Plasma Model
CIRSOS	Software with ability to perform 3D internal charging simulations (Collaborative Iterative Radiation Simulation Optimisation Software)
DICTAT	Software for 1D Internal charging analysis (Dielectric Internal Charging Threat Assessment Tool)
EMAGS-3	An ESA study of Solar Array Triggering Arc Phenomena
FLUMIC	A worst case electron environment model for internal charging (Fluence Model for Internal Charging)
Gmsh	Software generator of finite element meshes
MCICT	Software for 1D Internal charging analysis (Monte Carlo Internal Charging Tool)
MOBE-DIC	A worst case electron environment model for internal charging (Model of Outer Belt Electrons for Dielectric Internal Charging)
NASCAP	Software for 3D simulation of surface charging (NASA Charging Analysis Program)
NUMIT	Software for 1D Internal charging analysis (Numerical Integration)
SCATHA	A spacecraft dedicated to surface charging observations (Spacecraft Charging at High Altitudes)
SPIS	Software for 3D simulation of surface charging (Spacecraft Plasma Interaction Simulation)
SPENVIS	Web service for space environment analysis (Space Environment Information System)

4
Surface charging

4.1 Fundamentals

This Section gives a brief overview of the most important physical mechanisms connected with the surface charging of a body which is exposed to the space environment. Some of the randomly propagating charged particles incident on the surface of the body are collected by the surface, while the others are deflected or re-emitted. The ratio between these two contributions depends on the surface material and on the energy and angle of incidence of the impacting particles. The collected particles can be seen as a current from the plasma environment to the satellite. Because negatively charged electrons have a higher mean velocity than positively charged ions the spacecraft usually tends to assume absolute negative potentials.

Besides the simple collection of charged particles, additional effects can lead to a re-emitted current from the surface. So, incoming particles are able to eject electrons from the surface material. This effect is called secondary electron emission (SEE). This process is energy dependent and for some materials the ratio of released electrons to incident electrons (SEE yield) can be greater than one. Depending on the considered material an SEE yield of more than five is possible. Generally, there is a peak in secondary electron emission between several 100 eV and a few keV. Ambient electrons with energy between the two crossover points (the two energies where the yield is 1) in the yield curve, tend to charge the spacecraft positive instead of negative. In addition to SEE, the UV component of sunlight is also able to release electrons from the surface in what is called the photoelectric effect. Both SEE and photoemission play an important role in limiting the negative charging of the corresponding spacecraft surfaces.

Besides these direct currents to and from the surface to the plasma there are currents between different surfaces through the grounding network of the satellite. Note that a small current can even bleed through the thin dielectric (insulating) surfaces and this can have an impact on the final current balance on these surfaces.

The charging process continues until an equilibrium condition is reached, which is characterized by a balance between all collected and emitted currents (positive and negative). In Figure 4-1 the main current contributions connected with the charging of a body in space plasma are depicted. At equilibrium the black and the blue currents are balanced.

The charging process is influenced by a lot of different physical effects defining and changing the surface currents as explained above. Additionally, the currents arising from the external plasma are changed by the spacecraft potentials which extend out into the plasma. Also currents flow from one part of the spacecraft to another through the grounding network.

Hence, when a realistic assessment of the charging threat on a satellite is performed, the use of a dedicated 3D simulation tool where all these effects are taken into account is essential. Note that there can be large differences between 1D/2D tools and a fully 3D simulation due to the influence of the charged spacecraft on the plasma creating sheaths which can only be considered in a 3D tool.

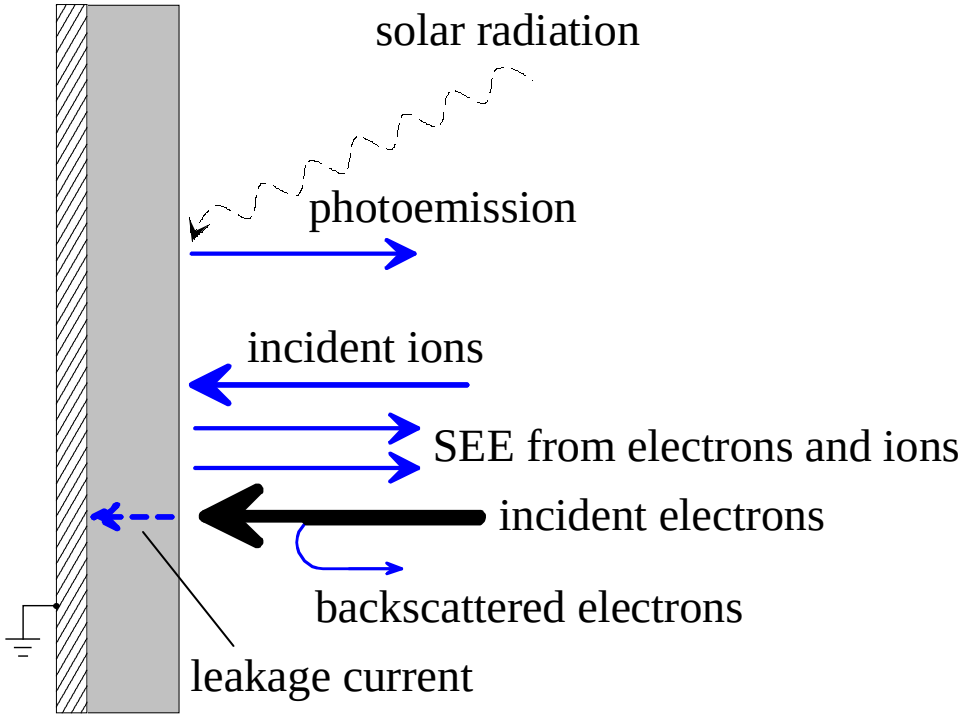

Figure 4-1: Current contributions influencing the surface charging of a body in space plasma

Surface charging and the corresponding effects and possible threats to the spacecraft functionality can be divided into two major processes:

- Absolute charging – this relates to the changing floating potential of the grounded parts of the satellite with respect to the ambient plasma environment. Usually, the time to reach equilibrium floating potential is very short, i.e. some milliseconds, because of the very low capacitance of the spacecraft w.r.t. the plasma environment. However, depending on the material distribution on the satellite this process can sometimes last longer, i.e. minutes, especially if the material distribution is dominated by dielectric materials.
- Differential charging - because of different material properties in terms of SEE and photoemission yields, different materials on the surface of the spacecraft tend to charge unequally. Differential charging can even occur between surfaces made of identical materials where one surface is sunlit and the other is in shade, or because of different potential barriers above these surfaces forcing secondary electrons to be recollected locally. For differential charging, it can take several minutes or hours to reach equilibrium. The timescale is ruled by the relatively high capacitances of spacecraft surface areas w.r.t. the grounded layers beneath. Differential charging is reduced by current leakage across the surface and through the dielectric thickness.

In eclipse conditions and for a low energy plasma equilibrium potentials in volts are usually on the order of two to three times the plasma energy in eV. These plasma conditions are usually encountered in the ionosphere and plasmasphere at low altitudes with low inclination below 50 degrees and are usually considered uncritical. In a very dense and low energy plasma the satellite absolute potential can be driven by the voltage of the space exposed interconnectors on the solar array. These are often positively biased with respect to spacecraft ground and attract electrons so that the satellite absolute potential becomes negative.

For LEO orbits with a high inclination, such as sun-synchronous orbits, the satellite has crosses the auroral zone where higher energy (~10 keV) electrons can be found. In this region, are found auroral

arcs where high energy electrons are streaming towards lower altitudes due to geomagnetic storms. Simultaneous with the arrival of these high energy electrons the cold background plasma density can also be greatly reduced in this region, producing a hazardous environment with a chance of strong satellite charging. In these auroral charging conditions the satellite potential can drop down to levels around -1kV with differential potentials that can also be rather high so that electrostatic discharges (ESDs) are possible.

Orbits around the earth above the ionosphere and plasmasphere are mainly characterised by plasma with a small total density. The energy distribution of this plasma varies as a result of changing geomagnetic configurations and due to the injection and subsequent decay of hot plasma during geomagnetic substorms. Hence the range of possible potentials in the outer magnetosphere is also wide. When secondary and photoemission effects dominate, the satellite potential is close to 0 V but for worst case conditions with a large amount of electrons at high energies, well above the second cross-over point in the yield curves, charging to very high negative potentials, in the range of -10 kV, is possible. If insulating satellites surfaces are used there can also be a high potential difference between sunlit and shaded surfaces due to the photoemission which cannot be balanced between insulating surfaces.

4.2 General methodology of surface charging analyses

4.2.1 Introduction

Since there are many aspects of the space environment that can have a detrimental effect on a spacecraft or its operations, it is part of the spacecraft design process to make an assessment of how severe the effects can possibly be. These analyses require an understanding of the environment and can involve testing in the laboratory, computer simulation or both. Where space systems are re-used in the same or a similar environment, heritage can also be relevant

Spacecraft surface charging has a strong dependence on the complete spacecraft geometry. Although individual exposed structures and materials are often tested in the laboratory under charged particle irradiation, realistic laboratory testing of a whole spacecraft is seldom possible and so computer simulation plays a very important role.

In this Section we discuss the general requirements and methods of surface charging analyses.

4.2.2 Necessity of 3D surface charging analyses

The first decision which needs to be taken in a new project is on the necessity of a dedicated 3D surface charging analysis. The flowchart given in Figure 4-2 shows the corresponding decision tree which is usually followed to determine if a 3D analysis is performed. So, it is important to consider whether the satellite is launched into a critical orbit (GEO, MEO, GTO, Polar) where surface charging and possible ESD can occur. In such a case it is strongly recommended to perform a charging analysis to show the robustness of the satellite design with respect to the plasma environment. The same is recommended if special requirements with respect to charging are applicable for the mission, e.g. scientific missions with requirements for the maximum allowable differential potential on the satellite.

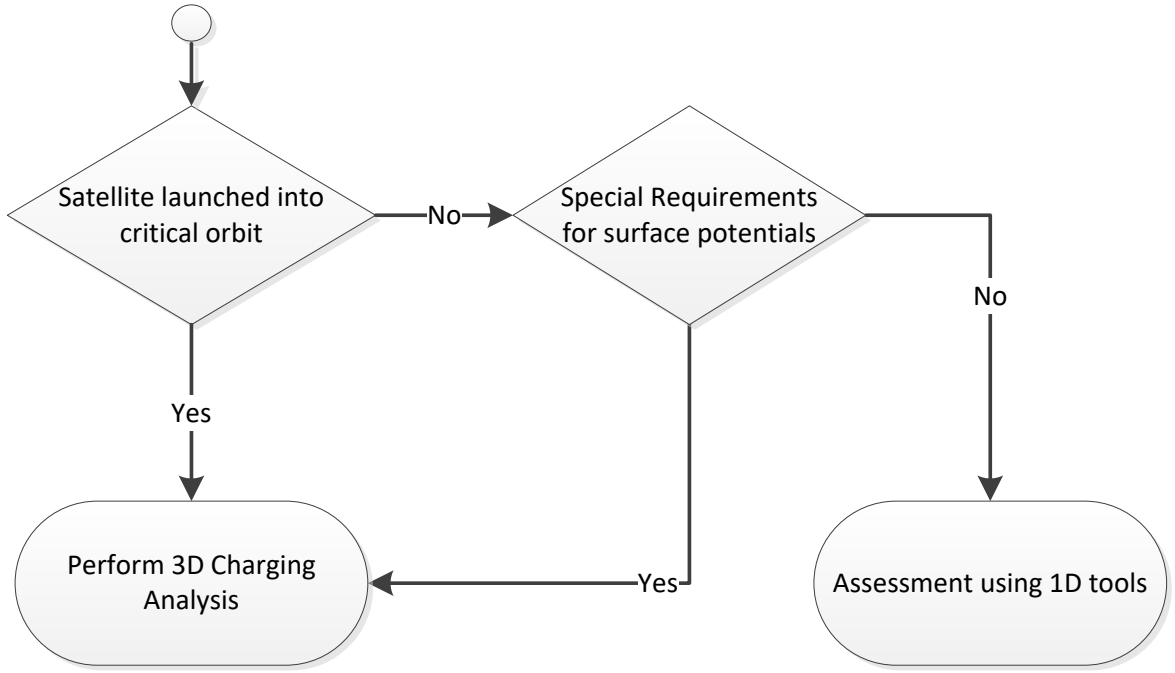

Figure 4-2: Flowchart showing the steps needed to determine the necessity of a 3D surface charging analysis

4.2.3 Simulation process

The typical analysis process including the necessary inputs and outputs and interpretation of results is shown in Figure 4-3. The main inputs for the 3D analysis are the basic electrical circuit of the satellite along with a dedicated 3D CAD model with the most important space exposed surface materials included. The plasma environment definition coming from the project specific environmental specification or the applicable standard (usually ECSS-E-ST-10-04 [RD.2]) is also an important input to the analysis.

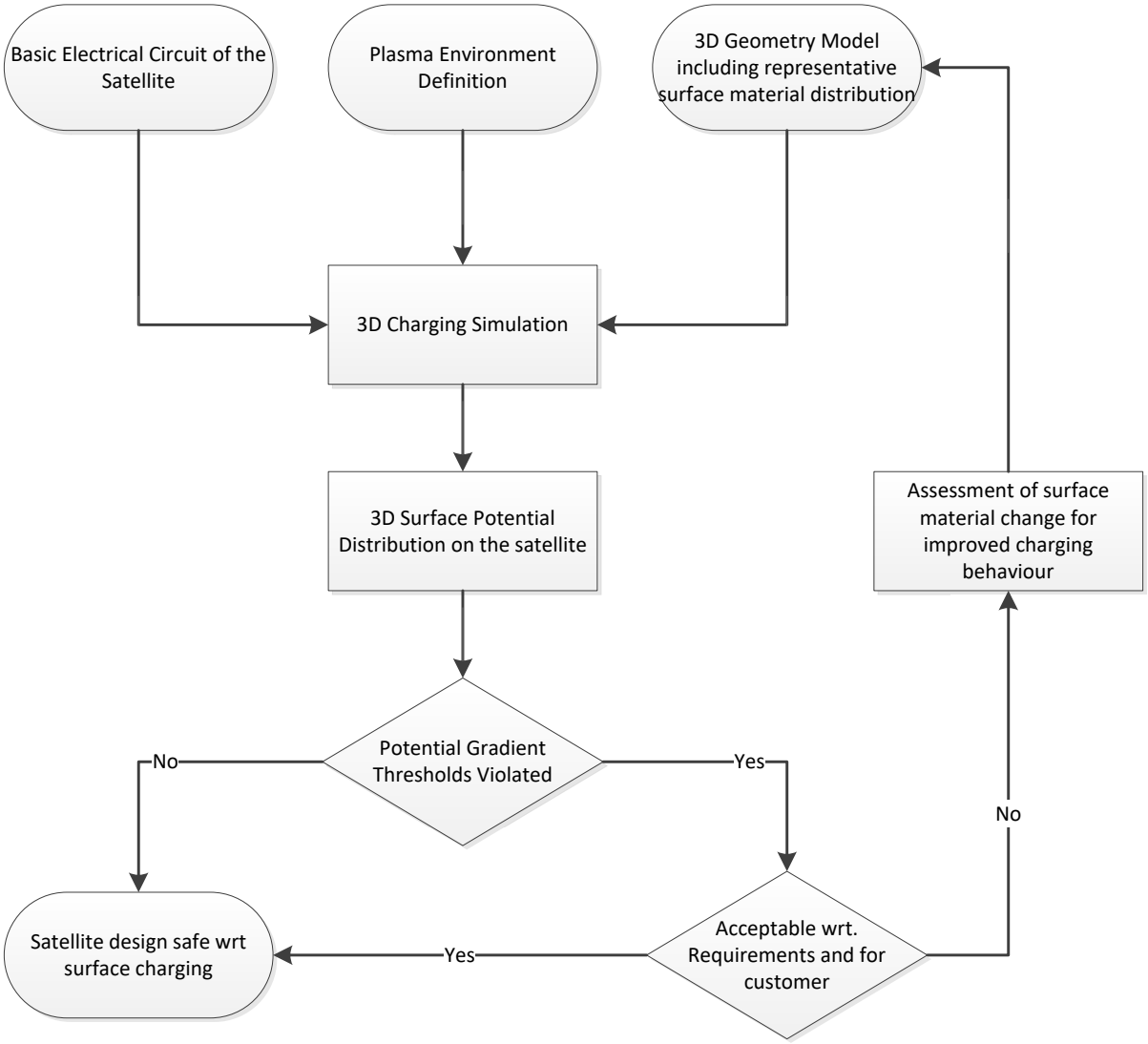

Figure 4-3: Flow diagram of the typical process of a 3D charging analysis

4.2.4 Assessment of simulation results

The main output of the analysis is the surface potential distribution on the 3D model of the satellite which can then be used to determine the potential differences to be expected on the satellite. Maximum differential potentials for dielectrics with respect to ground or an adjacent metal are then compared against the generic requirements for the onset of ESD given in ECSS-E-ST-20-06:

- Where the conductor is positive with respect to the dielectric ('normal potential gradient')
- Where the conductor is negative with respect to the dielectric ('inverted potential gradient')

When special requirements which are more stringent than the generic ones, for the satellite are applicable then it is important to use these requirements in the assessment of the results. If the applicable thresholds are not violated the analysis is finished and the satellite design with respect to surface charging can be consolidated. If the thresholds are violated there are in principle two options:

a. The design of the satellite can be changed in order to get a better charging behaviour e.g. by using more conductive materials or changing to materials with higher SEE yield. The effectivity of the proposed design changes is then verified by an update of the charging analysis taking the changes into account.

b. If a design change is not possible or easily done there is also the possibility to prove that the violation of the requirements poses no major threat or impediment to the satellite mission. In this case the ECSS procedure requires that the customer is involved in the acceptance of such a non–compliance.

4.3 Electrostatic discharge

4.3.1 ESD types

There are different basic types of ESD, depending on the materials which are involved in the event.

- 'Metal ESD' is a direct discharge between two conducting parts of the structure. Due to the very good conductivity of the materials involved the ESD pulse is very fast discharging the elements, which leads to very high peak currents. The very high current can cause permanent damage to the involved materials and in combination with the short pulse duration strong electromagnetic interference can be created which can disturb other systems on the satellite. Due to these dangerous properties metal ESDs are generally prevented on a real system by means of grounding of all conducting parts to the structure.
- A 'triple point' where metal, dielectric and vacuum come together is particularly associated with strong ESDs. It can become a discharge site when an inverted potential gradient (IPG) arises, i.e. where a conductor is more negative than an insulator. A strong electric field can exist between the negative metal and the less-negative dielectric. Electric field-induced electron emission is initiated from an irregularity on the metal surface and the electrons impact the adjacent dielectric. If the impact energy is sufficient, there is secondary emission which drives the dielectric positive and increases the electric field between metal and dielectric which further increases the electron emission from the metal in a run-away process. Triple point discharges can lead to 'flash-over' (described in Section 4.3.3)
- Other discharges are dielectric material discharges (as described in ECSS-E-ST-20-06) which include surface propagating discharges that can be triggered on dielectric coatings by punch-through of the dielectric.

4.3.2 Thresholds for ESD occurrence

Depending on the exact situation there are mainly three different threshold values defined for the onset of ESDs:

- The straightforward value is the material specific dielectric breakdown field strength. If this threshold is reached the charge stored on top of an insulator is released to the conducting layer beneath. This is a discharge event where the transient goes through the material. If the exact value for the dielectric breakdown voltage or field strength is not exactly known, ECSS-E-ST-20-06 clause 6.2.1 gives a default value to be used.
- Two other types of discharges involve dielectric surfaces:
  - Direct potential gradient ESD, where the dielectric surface is at a more negative potential than an adjacent conducting one. In this case of the threshold for the risk of ESD is given by ECSS-E-ST-20-06 clause 6.2.1.
  - Inverted potential gradient (IPG) where the conductor is at a more negative potential compared to the insulator. In this case the threshold value is lower because field emission of electrons from the conductor plays an important role in the triggering of the ESD.

Concerning the exact value for the onset of ESDs in this scenario the literature values differ. The ECSS-E-ST-20-06 standard gives one value [clause 6.2.1], whereas NASA literature [RD.22] states a slightly different value.

4.3.3 Quantitative characterization of ESD electrical transients

Several important parameters can describe characteristics of a discharge transient relevant to the assessment of the criticality of the ESD: total amount of stored charge on the surface Q; the amount of released energy E_{rel}; the rise time τ_r; the half width of the pulse $t_{HW;}$ and the peak current flowing during the discharge I_{max}.

Here we focus here on inverted potential gradient ESDs. At the position where the ESD is triggered a cathode spot is created where high current causes local plasma emission. This plasma expands from the spot and forms a conducting bridge to the other parts of the insulating surface. Due to this plasma expansion it is possible to discharge the whole charged surface. The rise time and the pulse half width are directly connected with the propagation velocity of the plasma front.

Following this theory, the characteristic values of a possible ESD can be estimated following different models reviewed by Inguimbert et al. 2017 [RD.23]. This reviewed the three types of models that have been developed to reproduce the flash-over expansion: the perimeter theory, PIC methods, and the plasma bubble expansion semi-analytical model.

The perimeter theory is an analytical method which has been first developed to reproduce the shape of the flash-over and explains its extinction: see Amorim et al., 2005 [RD.24], R. Briet, 2005 [RD.25], Ferguson and Vayner, 2013 [RD.26]. This theory can be summarized by considering the charged insulating surface as a plate capacitor with a capacitor according to the following equations:

$C = \varepsilon_0 \varepsilon_r \cdot \frac{A}{d}$	Equation 1

where ε0 is the permittivity of free space, εr is the relative permittivity of the dielectric material, d the thickness of the coating and A the surface area. Using the capacitance according to equation 1 and the potential difference from the charging simulation U0 the charge stored on the surface is given as

$Q = C \cdot U_0$	Equation 2

The ESD stays alive as long as the potential difference which triggered the event is high enough. A direct consequence of this fact is that only a fraction κ of the total charge stored on the surface is released with the ESD. This value is usually on the order of (30 – 50) % but can reach up to nearly 100 % in worst-case conditions such as experienced during the EMAGS 3 project on a full size solar array (4 by 2 square meters). As a results, in the analysis described in the following equations, it is important to assume a value of 100 % (κ =1). Note that EMAGS3 always saw a discharge before the inverted potential gradient had exceeded 500 V to 600 V. The total amount of energy released during the ESD can be calculated by taking the difference between the stored energy before and after the discharge event:

$$E_{preESD} = \frac{1}{2} \cdot C \cdot U^2 = \frac{Q_{preESD}^2}{2 \cdot C}$$	Equation 3

$$Q_{rel} = \kappa \cdot Q_{preESD} \rightarrow Q_{postESD} = Q_{preESD} - \kappa \cdot Q_{preESD} = Q_{preESD} \cdot (1 - \kappa)$$	Equation 4

$$E_{postESD} = \frac{Q_{postESD}^2}{2 \cdot C}$$	Equation 5

$$E_{rel} = E_{preESD} - E_{postESD} = \frac{Q_{preESD}^2}{2 \cdot C} - \frac{\left(Q_{preESD} \cdot (1 - \kappa)\right)^2}{2 \cdot C} = \frac{Q_{preESD}^2 \cdot (1 - (1 - \kappa)^2)}{2 \cdot C}$$	Equation **6**

For the calculation of the rise time and the half width of the ESD, assumptions about the shape of the current pulse are made. The approximation of a triangular shape for the current is a reasonable approximation. Due to the plasma front propagation the area included in the discharge process increases quadratically with time, if a circular shape of the plasma expansion is assumed. Since the amount of charge is proportional to the area, the charge included in the discharge process rises also quadratically leading to a linear increase for the current of the pulse with time. The peak current for the triangular ESD pulse is

$$I_{\max} = \frac{\kappa \cdot Q}{t_{HW}} = \frac{\kappa \cdot C \cdot U_0}{t_{HW}}$$	(Equation 7)

The pulse half width can be estimated as

$$\frac{R_{\min}}{v_P} \leq t_{HW} \leq \frac{R_{\max}}{v_P}$$	(Equation 8)

where Rmin and Rmax stand for the geometrical widths of the charged surface (see Figure 4-4).

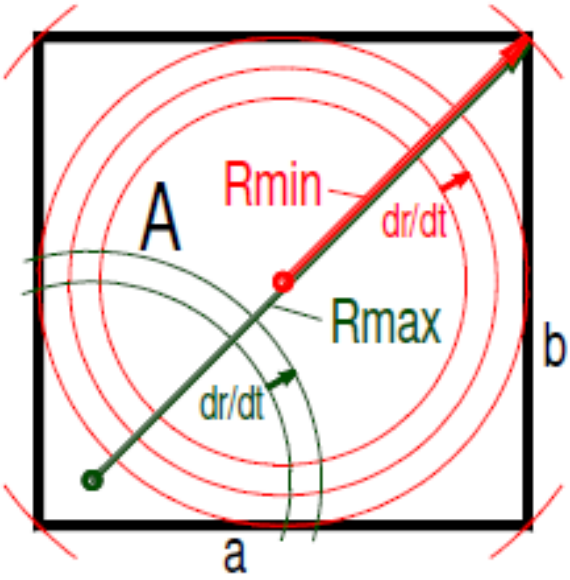

Figure 4-4: Charged surface with area A showing the geometrical meaning and the range for the parameter R

More complex and more physical models have been developed based on Particle-in-Cell methods but they require long calculation times to get good statistics: see Roussel et al., 2012 [RD.27], Young and M. W. Crofton, 2016 [RD.28].

Finally, as part of the EMAGS-3 project, Sarrailh et al., 2013 [RD.29] developed a semi-analytical model of electrostatic discharge on a solar array with the following characteristics.

When blow-off, which emits electrons, has emptied the charge stored by the satellite capacitance and reduced the satellite potential to zero volts, the plasma bubble expands isotropically at constant velocity.

Within the plasma bubble the dielectric potential on the solar array surface is instantly neutralized. Outside the bubble, electrons which are emitted from the bubble are collected by the solar panel. The current emission is uniform at the bubble surface and limited by space charge. The collected electrons create secondaries but these have low energy and are recollected locally. Hence the model treats only backscattered electrons which are able to redistribute current across the surface. The flash-over current collected by the solar array strings is the total electron current, i.e., electrons extracted from the bubble minus the back-scattered current. The potential on the array varies due to the net current collected.

For the calculation of the rise time and the half width of the ESD following the flash-over plasma bubble expansion model, one needs to discretize large dielectric areas in 2D, such as solar panels, using a regular mesh described in the next figure. The cell matrix is composed of n lines and m columns. Each cell $Cell_{i,j}$, where $i \in [1, n]$ and $j \in [1, m]$, has its own voltage $V_{i,j}$ and collected current $I_{i,j}$. Integrating the current density on lines and columns provides information on the current raise and fall during the flash-over.

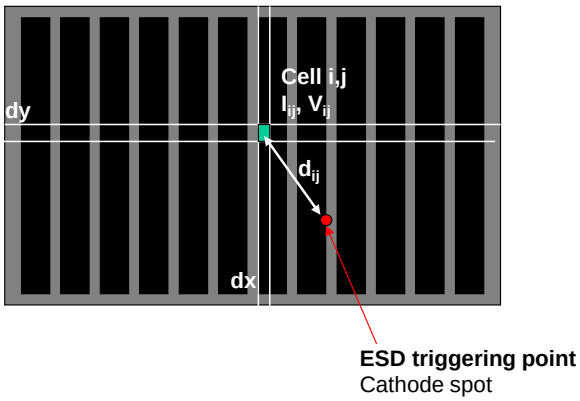

Figure 4-5: Two-dimensional meshing of a solar array (from Sarrailh et al 2013 [RD.29])

This model is the most adapted to flash-over current prediction on solar arrays because it represents the physics behind it and requires a limited number of inputs (size of solar arrays, location of ESD trigger point and atomic number of the materials composing the plasma bubble).

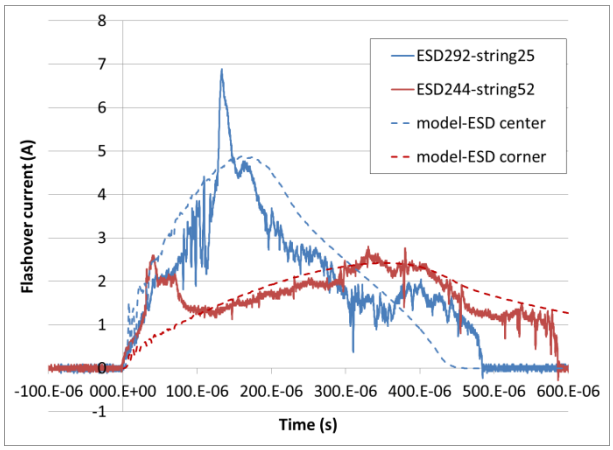

The first example in the centre of the panel and discharging the total charge of the surface and another discharge occurring in the corner of the panel and partially neutralizing the panel.

Dashed lines are current from the model of Sarrailh et al. 2013 [RD.29].

Figure from Inguimbert et al 2017 [RD.23].

Figure 4-6: Examples of 2 discharges

The plasma bubble expansion model has been used to size the flash-over simulator used for ESD and arcing tests at ONERA [RD.30], [RD.31].

4.3.4 Interpretation of results

The results calculated using the full plasma bubble expansion model or the simplified formulas given in 4.3.3 can be used to judge the criticality of the possible ESD. In this frame it is important that the calculated energies and peak currents are compared against the levels to which the equipment in the vicinity of the arc site are tested. This ensures that no permanent damage can be caused by the corresponding discharge.

Additionally, the pulse width along with the peak current can help to roughly estimate the spectrum of the electromagnetic interference emitted by the current pulse which then can provide information for a further analysis of possible disturbances of sensitive systems caused by the discharge. The overall shapes of the discharge currents, described in the previous chapter, do not give the high frequency variations that are dependent on the microscopic details of the discharge process.

If the charging analysis predicts the possibility for ESDs on the solar array it is important that the solar array electrical design is checked against the robustness against discharges with the most important fact that no sustained arcs are possible. There are well known best design guidelines for this task given in [RD.6] and [RD.7].

Additionally, possible design changes of the surface materials can be performed which can help to reduce the amount of surface charging and especially differential charging. These changes and the corresponding impact on the charging of the satellite are usually checked by a corresponding update of the analysis to be able to see the impact and to be able to perform a trade-off between the different options.

4.4 Critical aspects with respect to worst case surface charging analyses

4.4.1 Orbit

First of all it is important to identify the environment of the satellite orbit in which the satellite is launched. The criticality of the environment is mainly driven by the satellite orbit. There are in principle three different orbits where it is usually considered mandatory to perform a charging analysis. These orbits are LEO polar orbits with an orbit inclination above 60 degrees and all GEO, GTO and MEO orbits.

High surface charging levels are commonly observed in the outer magnetosphere including GEO. Here hot plasma (several 10s keV) can be found and there is little cold plasma to mitigate its charging. A series of severe environments associated to large charging levels measured in flight are available in the literature, see Annex A. In GEO, all of them can be considered isotropic. Anisotropy of the charging environment is only caused by the sun orientation.

For the LEO case the most critical surface potentials are seen under eclipse conditions. In LEO polar orbits the plasma environment is usually composed of cold background plasma accompanied, during crossings of the auroral zone, by high energy electrons from the outer magnetosphere and streaming down to low altitudes along magnetic field lines, particularly during geomagnetic storms. For the dense background plasma, the satellite, moving at typically 7-8 km/s in LEO, is supersonic with respect to the thermal velocity of the ions. This leads to a ram/wake effect for the ions which causes increased collection of ions on the front surfaces while the ion collection on the rear surfaces is lowered. Additionally there is a strong variation of the ion current on the side parts of the satellite where the ions kinetic velocity is combined with the satellite velocity. It is important for a worst case charging simulation that these effects are taken into account.

The key aspects of spacecraft charging at MEO are almost the same as in GEO. Charging environments are at least of the same order of magnitude as in GEO [RD.32], [RD.33]. It is important to pay attention in this orbit to frequent eclipse exits.

4.4.2 Material properties

Besides the satellite geometry the surface material distribution on the satellite is crucial for a sophisticated analysis or simulation of the worst case potentials on the spacecraft. The main parameters which are important to know and are fed into an analysis are the surface and bulk conductivities of the materials as well as the dielectric constant and atomic number. Also required are the parameters used to describe the secondary electron emission by electrons and protons, the photoemission of electrons as well as the correct characterization of the effect of radiation induced conductivity. If these parameters are missing for materials covering large percentages of the total satellite surface a parameter variation, especially for the maximum secondary electron emission yield, can be performed to work out the impact of this parameter on the results.

Dielectric resistivity favours spacecraft absolute charging, especially considering dielectrics in Sunlight because they limit the amount of electrons released from the spacecraft ground structure to the environment (by photoemission). Dielectric resistivity however changes with time (ageing effects) and with the environmental conditions, especially when submitted to high energy electrons capable of generating Radiation Induced Conductivity (RIC). RIC is important for thin insulators located at the spacecraft surface and the bulk resistivity can decrease by one or two orders of magnitude at least. This process needs to be taken into account for precise estimation of absolute and differential voltage.

4.4.3 Sunlit/Eclipse

When Sunlit, fully conductive spacecraft generally do not generally charge significantly because electron photoemission prevails at GEO with respect to severe electron fluxes. However, spacecraft with a significant amount of sunlit surfaces covered with dielectric materials can charge very negatively. In such cases, the spacecraft grounded structures can collect a larger amount of electrons from the ambient environment than it emits by photoemission and secondary emission by electron impact. It results in negative charging of the structure while sunlit dielectric tends to stay close to zero potential. This situation is critical since high voltage gradients can occur on sunlit dielectrics and trigger electrostatic discharges, especially on solar panels covered with insulating cover glasses. It is worth noting that sunlit dielectrics are generally prevented from staying very close to zero volts in a long debye length plasma, during strong charging events because of three-dimensional negative barriers of potential imposed by the surrounding negative spacecraft surfaces. As a result, these sunlit dielectrics also reach a negative potential, although still positive with respect to the spacecraft ground. This is the so-called **inverted potential gradient situation**, known to be the most risky in GEO. In brief, a harsh electron environment can produce significant differential charging on GEO spacecraft if the spacecraft exposes a relatively small area of conductive parts to the sunlight.

Two specific situations arise from this effect:

a. Spacecraft in sunlight with few grounded conductors facing the Sun. For a given spacecraft, this depends on the position on the orbit. For example, large conductive antenna reflectors can play an important role, and charging can strongly depend on the MLT.

b. Eclipse exit. A long eclipse gives the opportunity for the spacecraft to charge highly negatively because of the absence of photoemission. In addition, dielectrics cool during eclipse which can reduce their conductivity. At eclipse exit, the progressive exposure to sunlight generates a transitional situation with the possible creation of or increase of the inverted gradient potential, especially on solar panels.

4.4.4 Protons

An additional key effect is charge reduction by proton fluxes. At GEO, energy proton flux is strongly enhanced by strongly negative spacecraft charging because the Debye length is large, permitting the collection of protons with large impact parameters. The Orbit Motion Limit theory predicts an increase in the proton current density by a factor 1+e*phi/KT where phi is the spacecraft potential and KT the proton population temperature (assuming a Maxwellian distribution). In addition, secondary electron emission under proton impact can exceed unity for protons of some keV energy. This combined and multiplicative effect is efficient at limiting negative spacecraft charging below or around -10 kV.

4.4.5 Electric propulsion

The presence of an electrical propulsion system almost always has a major effect on the spacecraft charging state. EP systems generally have a neutraliser which effectively clamps the spacecraft ground to relatively low potentials with respect to the ambient space plasma. Transient effects during switch-on can however cause temporary high differential charging. Also the EP grounding configuration, can influence the spacecraft floating potential. Charge exchange ions can also be re-collected by the spacecraft and affect the surface potentials and modify surface properties. Differential charging can still occur if dielectric surfaces are shielded from the emitted plasma.

4.5 How to set up a simulation

4.5.1 Charging environment parameters

Worst case charging environments can be found in ECSS-E-ST-10-04. This standard gives two normative environments [see Annex A for details]:

- A severe geostationary environment based on an extreme charging even on SCATHA
- A severe auroral charging environment based on an extreme DMSP charging event. Two forms of this are presented – the original distribution function from Yeh and Gussenhoven, 1987 [RD.9] and a Maxwellian fit to the same distribution function proposed by Imhof et al 2016 [RD.8]. Note that this auroral environment is expected be a worst case for only up to 10 s, even though an auroral crossing can be up to 2 minutes.

Annex A includes details of other severe charging environments.

4.5.2 Modelling requirements for surface charging analyses

0D analytical and 1D tools can be used for rough estimation of spacecraft surface charging in the very early stages of spacecraft design. They generally assume simplistic geometries and a limited number of materials for the structure and covering dielectrics.

It is recommended to use 3D tools for a realistic computation. SPIS and NASCAP are widely used. Not all codes are equally capable. In order to guarantee that the simulations using a 3D simulation tool are representative, it is important that the software that is used is able to take into account the following effects:

- Plasma modelling by PIC and fluid models in order to calculate the currents from the plasma towards the spacecraft as well as potentials in the simulation volume

- Calculation of photoemission currents
- Calculation of secondary electron emission by electrons and protons
- Calculation of backscattered electron current
- Basic model of the electrical circuit of the satellite
- Computation of radiation induced conductivity. Surface and bulk conductivity of the materials involved

The following are the minimum outputs required from the 3D simulation

- Time dependent potential evolution on the various surfaces of the satellite; averaged and ideally special selectable areas; differential potentials between local dielectric surfaces and the satellite structure potential
- Time dependent plots of the various current contributions on the different surfaces
- 3D spatial plots of the surface potential distributions for selected times
- 3D spatial plots of the various current contributions on the surfaces
- 3D plasma volume potential plots
- 3D plots of particle densities (mainly interesting for sanity checks and special questions)

For LEO, the short Debye lengths tend to make simulations slow compared to GEO spacecraft. However, there are some simplifications that can make the simulation more efficient:

- No secondary particle dynamics are needed (in comparison to GEO where this is essential)
- For worst case auroral charging the modelling of the solar array interconnectors is usually not needed since for high negative charging there is no longer an attractive potential of the interconnects wrt to plasma
- Limit the simulation time to a time corresponding to the duration of enhanced charging environments based on the worst case environment definitions given in ECSS-E-ST-10-04 and Annex A. A realistic spacecraft capacitance needs to be used.

The remainder of this Section concentrates on summarising the simulation settings to be used when using the Spacecraft Plasma Interaction Software, SPIS (www.spis.org). For more details, see the SPIS Software User Manual [downloadable from http://dev.spis.org/projects/spine/home/spis].

4.5.3 Spacecraft geometry modelling

For efficient 3D computations, it is recommended to perform a trade-off between detailed and rough surface descriptions. It is important that elements that are included are representative of the global behaviour of the spacecraft potential with respect to the environment and of the local behaviour of sensitive elements. For appropriate spacecraft absolute charging, it is recommended to merge large surfaces with globally the same properties (e.g. radiators, solar panels) giving them the properties of the main component. For small elements, it is recommended to build an envelope surface (e.g. instruments).

For some missions, even small pieces of conductors can significantly modify the spacecraft worst case potential. This is for instance true for scientific missions dealing with low energy plasma measurements where solar panels interconnects are known to modify significantly the plasma collection. It is important to make the effort to account for these currents without necessarily meshing at small scale, for instance through analytical, semi-analytical, multi-scale coupled approaches.

The points below need attention to ensure a realistic simulation:

- Roughly correct areas of correct materials
- Merging of surfaces on one panel, e.g. if there are several radiator surfaces on the same panel they usually can be merged into one surface with the same area which eases the meshing
- Approximate shape, e.g. size of solar arrays, ratio of sunlit to eclipse areas, self-shadowing. In GEO, features on a surface less than 1/20 of the surface dimension can probably be simplified.
- Small connecting rods can be omitted, e.g. the solar array struts can be ignored as long as the electrical connection of the array to the rest of the spacecraft is included.
- Antennas and solar arrays can be represented by 1D and 2D cylinders and planes in SPIS.
- Combining many small areas of a material into a few large areas can be done if it does not change the physics of current collection from orbit motion limited to space-charge limited (thick sheath to thin sheath). An example is the solar array interconnects in a plasma with a Debye length similar in size to the interconnect dimension – these can instead be simulated by a user-defined current-voltage relationship.
- For LEO a good representation of the conductive area in the ram direction is important

4.5.4 Gmsh – The CAD interface to SPIS

The SPIS software uses Gmsh to build the CAD and the mesh of both spacecraft surface and computational volume. It follows the BRep (boundary representation) approach where the user defines first the nodes of the geometry. Based on these node definitions the lines, circle arcs or ellipse arcs connecting the nodes are then defined. This definition is possible using the text editor or directly with the Gmsh interface. The lines and circle or ellipse arcs are then used to define the boundaries of planar or curved surfaces. Again, this definition can be performed by adding the corresponding commands in the geometry file (*.geo) or by using the GUI of the tool. For surfaces which are completely contained in another surface (e.g. radiator contained within a larger MLI area) it is important that these small surfaces are modelled as holes in the large surface. Physical surfaces are defined, made up of one or more geometrical surfaces with the same physical properties.

For a SPIS simulation to be correctly set, it is mandatory to define a volume enclosed by a **closed inner surface** (the spacecraft) and by a **closed outer surface** (the external boundary plasma limit). The computational volume is defined selecting the outer boundary first and afterwards the spacecraft needs to be selected as a hole in the volume, so that no mesh cells are generated inside the spacecraft. Note, that in case more than one satellite element is modelled, it is important to define all these elements as holes in the volume. The geometrical volume is defined as Physical Volume. This can be achieved through Gmsh.

If the finalisation of the SPIS simulation fails before SPIS starts to run, then it is very often the case that the error lies in the geometric model, e.g. missing physical surfaces, holes in surfaces not identified correctly.

The outer boundary is set up at a sufficient distance from the inner boundary in order to limit boundary condition side effects. Typically, the distance is several times the Debye length and several times the spacecraft dimensions. The GEO Debye length is often greater than one hundred meters. The electric field is thus similar to a spacecraft immersed in vacuum. In this case, it is not necessary to mesh a domain of several hundreds of meters, if using appropriate boundary conditions for the potential variation at the boundary (1/r decrease, where r is the distance to the spacecraft). In LEO, the spacecraft wake extends over a distance equals to a few times the spacecraft cross section for the

drifting ions. This domain is included inside the computational volume, unless an appropriate boundary condition is used.

The following example describes a simple cubic spacecraft body and a solar panel. The definition of points and lines is illustrated in Figure 4-7. The surface and volume definition with Gmsh for the is presented in Figure 4-8. The resulting surface and volume meshes are presented in Figure 4-9. Mesh refinement is controlled by a fourth parameter defining the size of the mesh grid following the three coordinates of each point of the CAD.

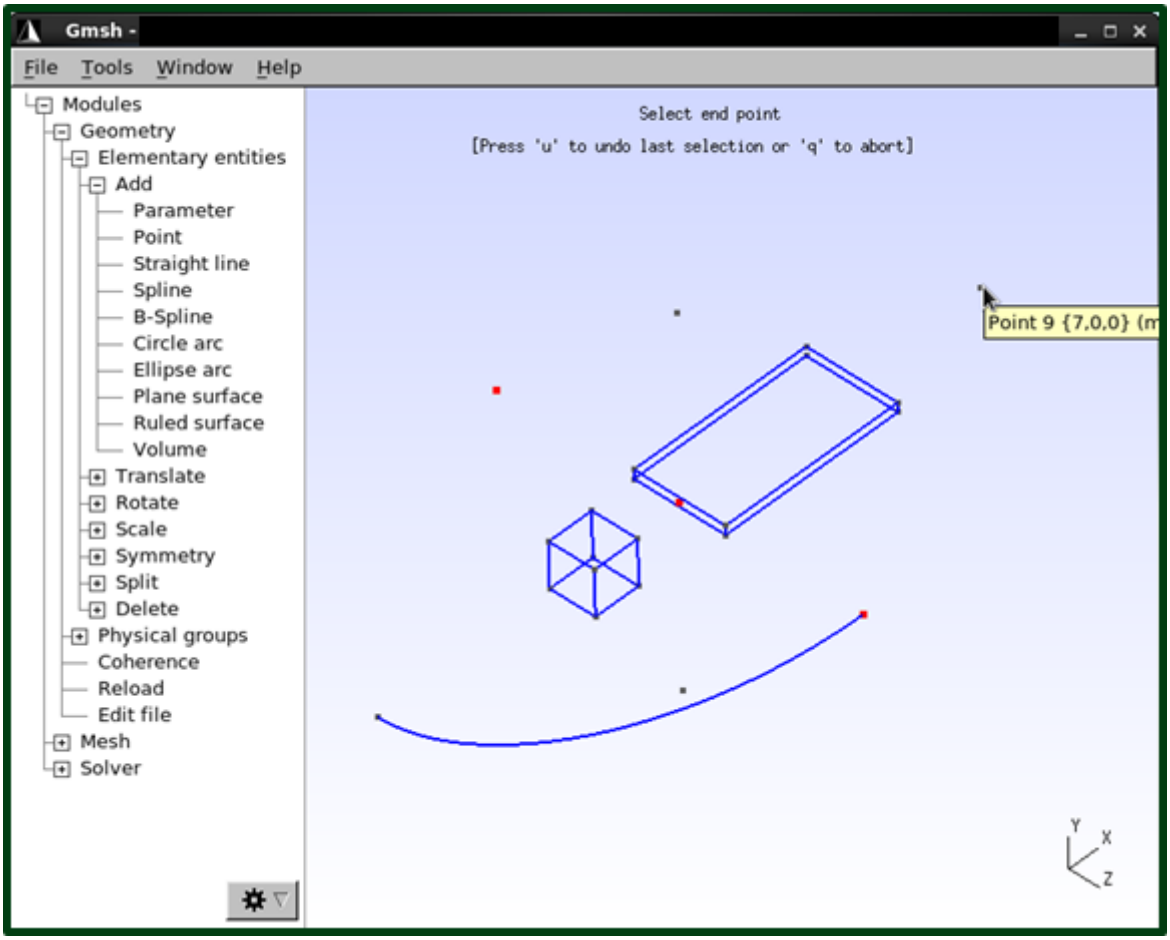

Figure 4-7: Definition of nodes and lines with Gmsh

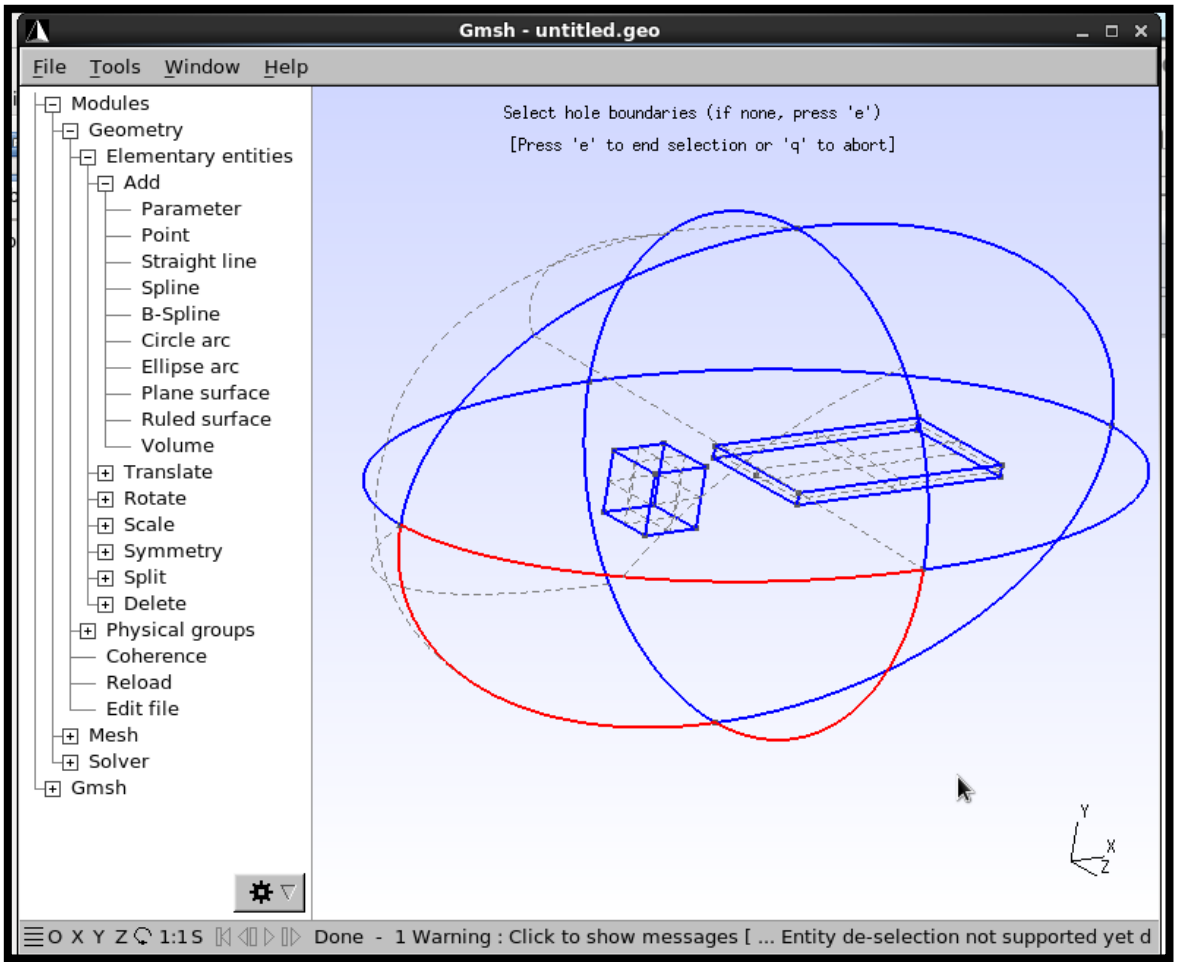

Figure 4-8: Definition of surfaces and volume with Gmsh

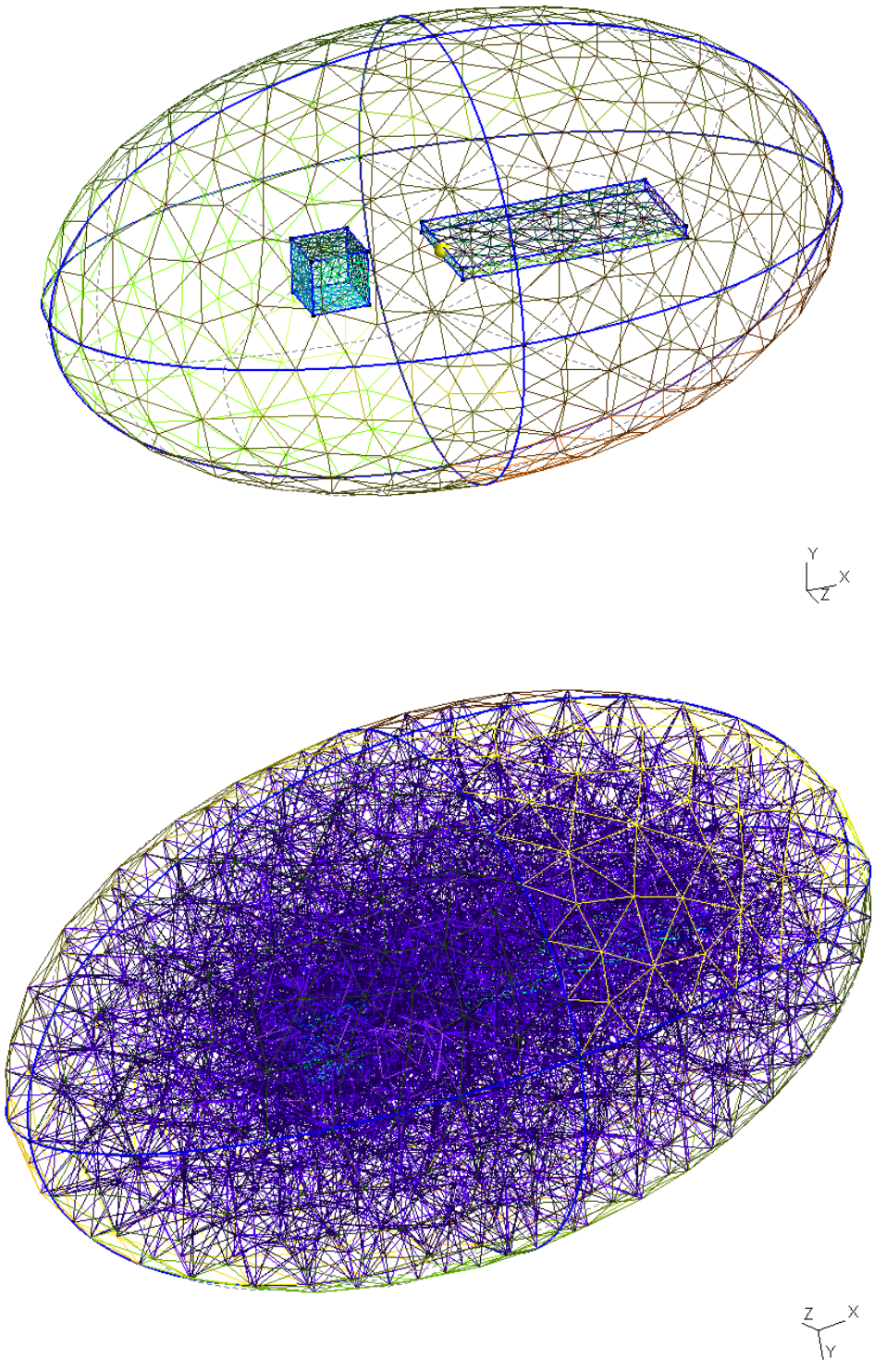

Figure 4-9: Top: Surface meshes of the spacecraft and boundary. Bottom: Volume mesh of the computational space.

4.5.5 Physical groups and surface materials definition

The interface between the Gmsh model and the SPIS software is controlled by the concept of the physical groups in the Gmsh file. So, it is possible to group the different elements - for 3D plasma simulations mainly surfaces and volumes, into so called physical groups. This concept allows the arrangement of all surfaces with the same physical properties into a dedicated group. Hence the number of different elements for which physical properties are defined in the software can be reduced.

It is important for a valid SPIS simulation to include groups for: the outer boundary surface, the different spacecraft surfaces, and the simulation volume of the plasma.

The physical and numerical properties of the spacecraft surface materials are set within the SPIS framework shown in the Figure 4-10. In this menu the type of group as well as the physical properties can be assigned to the physical groups previously defined in the geometry definition. For typical models there are in principle 3 types of elements available:

- Surfaces on the satellite
- Surfaces on the outer simulation boundary
- Simulation Volume

For the assignment of material properties to the spacecraft surfaces there is a pre-defined material library included in the software from which by drop-down menu the corresponding material can be selected. Additionally, it is possible to expand the materials list by defining other materials which can be needed for the simulation. In Figure 4-11 an example of the SPIS default material parameter list is given.

Besides the material properties and the global type of the group, an electrical node is assigned to the physical groups on the satellite. This assignment is important for the definition of the electrical circuit in the satellite. Both for post-processing analysis and numerical precision, it is very important to use a different electrical node for each group covered by an insulator. This is because of a surface potential smoothing which is performed across a node.

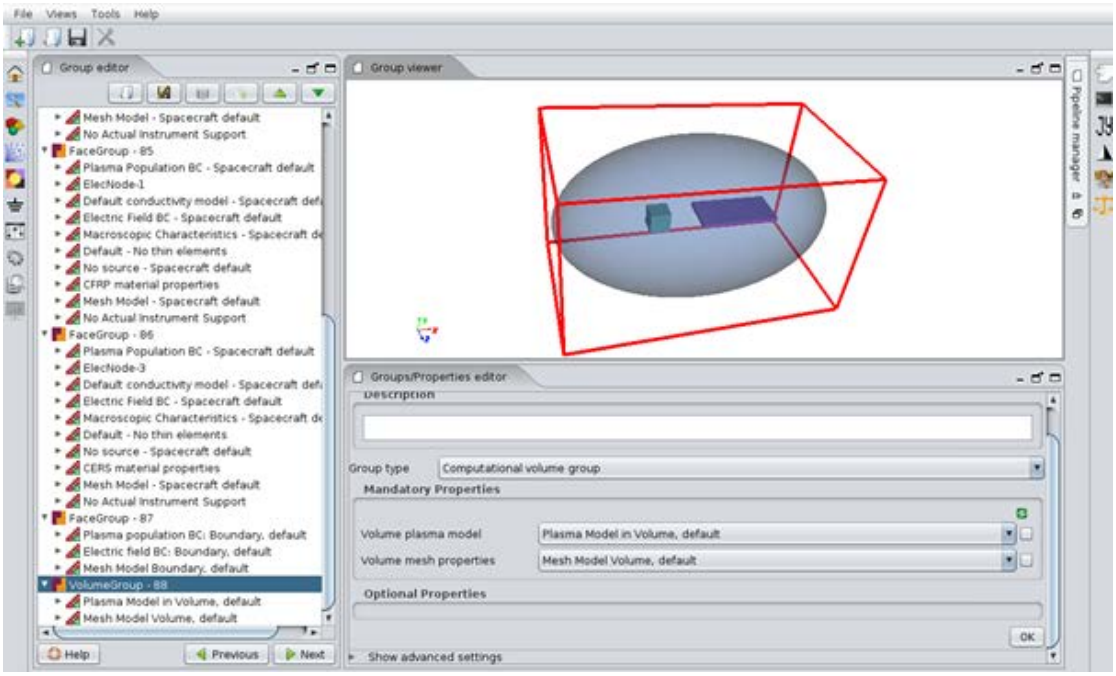

Figure 4-10: Definition of surface materials through the SPIS group editor

The basic material concept implemented in the SPIS software is comprised by a space exposed surface which is either conductive or non-conductive. However, it is always assumed that the inner surface of the space exposed material is conducting. This material concept is applicable for most of the standard configurations which can be found on satellites like MLI, radiators, paints and coatings on structural elements. However, there are some special cases where the model is over simplified.

Covering dielectrics are treated in SPIS as a thin layer with one face exposed to the environment and the other face grounded to the spacecraft potential. In this case, 1D capacitive and conduction circuit models are possible to be used to describe the evolution of the surface potential as a function of the spacecraft ground. This is included in SPIS material models used shown in the Figure 4-10.

For thick layers, when the dielectric thickness is not negligible with respect to the material size, 3D models of capacitive coupling and charge transport can be preferred to 1D models. This capability exist in SPIS-ESD and SPIS-IC but not in the current SPIS-GEO-SCI-DUST for surface charging. Also floating dielectrics for which both surfaces are facing the environment are not simulated and if required, specific ad-hoc models need to be developed.

The evolution of surface potentials needs to account for the interaction with the environment (collection and emission of particles) as well as conduction of charges stored on the surface of the dielectrics. Material properties can be described by a set of scalar or tabulated values, possibly at beginning, middle and end of life when data are available.

For a realistic simulation, the following input parameters are considered as necessary for each material:

- Photoemission current density at 1 AU from the Sun.
- Secondary electron emission yield as a function of impacting electron energy and incidence angle: it is important to use analytical laws with input parameters or tables coming from experiments. In case no such data is available, a sensitive analysis study is recommended by variation of the SEEE maximum yield parameters (yield and energy of this maximum).
- Electron emission by proton impact: it is important to use analytical laws with input parameters or tables coming from experiments. In case no such data is available, a sensitive analysis study is recommended by variation of the SEEP yield parameters (yield at 1 keV and energy of the maximum yield)..
- It is important that conductivity of surface dielectric takes, as minimum inputs, the bulk conductivity, the surface resistivity and the radiation induced conductivity.
- Dielectric constant, atomic number

An example of SPIS default material properties is given for polyimide in Figure 4-11.

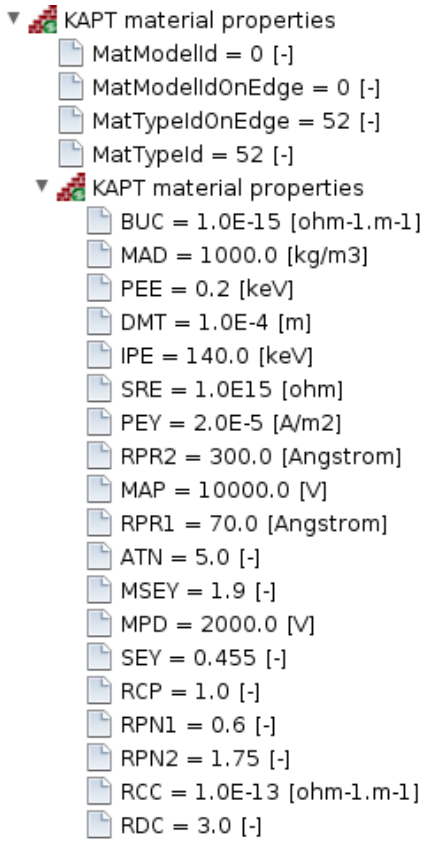

Figure 4-11: Example of material properties list used by SPIS

Remark: The dielectric thickness is controlled with MatThickness property and not by the parameter called DMT (dielectric material thickness, see Table 4-1. The DMT property is present to allow NASCAP properties lists to be imported easily into SPIS.

Table 4-1: Meanings of the material properties used in SPIS

Property name	Description
BUC	Conductivity
MAD	Density
PEE	E-Max of secondary electron yield curve
DMT	Thickness
IPE	Max dE/dx for protons
SRE	Surface resistance /square
PEY	Photocurrent at 1AU
RPR2	Range R2
MAP	Space discharge potential
RPR1	Range R1
ATN	Atomic number
MSEY	Delta-max of secondary electron yield curve
MPD	Internal discharge potential
SEY	Secondary yield for 1keV protons

Property name	Description
RCP	RIC power
RPN1	Range exponent E1
RPN2	Range exponent E2
RCC	RIC constant
RDC	Relative Dielectric constant

Materials which are not generally regarded as conductors but which have a relatively high conductivity, e.g. semi-conductive coatings, can be best represented in SPIS simulations as conductive. Otherwise there can be problems of very small time-steps leading to very slow simulations.

It is important to perform an analysis on the possible evolution of material properties with time spent in orbit. Three typical cases can be considered as of particular interest: BOL, MOL and EOL.

4.5.6 Basic electrical circuit of the satellite

The main connections between the satellite components are set up to describe the electrical grounding scheme. A typical example concerns the bleeding component resistor used to insulate the solar arrays structure with respect to the satellite body and to avoid permanent arcing in case of a solar cell insulation defect. Another example concerns plasma instruments with voltage bias with respect to spacecraft ground.

The electrical circuit is defined by a simple text file giving the type of connection (resistance R, inductance L, capacitance C or voltage V) followed by the two nodes which are connected and the value of the chosen connection type. The nodes used in this circuit definition are the nodes which are assigned in the group editor to the different physical groups. It is important to specify the electrical connections of every node. This can be by reference to spacecraft ground or to another node. However, circular definitions are not allowed and often a star shaped network starting from spacecraft ground (node 0) is sufficient.

Figure 4-12 gives an example where the solar panel identified by Id #1 is connected to ground of Id #0 by a 50 kOhm resistor, while other groups identified by ID #2 and #3 are grounded to the satellite structure (zero voltage).

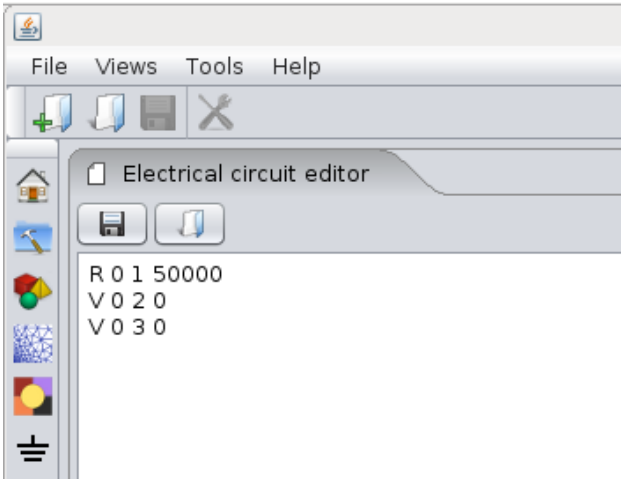

Figure 4-12: SPIS configuration of satellite electrical connections

4.5.7 Plasma models

Hybrid and analytical models of plasma density and current collection by the surfaces are recommended for estimating spacecraft charging levels within a reasonable amount of computational time. Fluid electrons are preferred up to now due to advantages in terms of memory and computation time. It is important to model ions using the PIC method when their drift velocity is large so that the ram/wake effect can be taken into account.

SPIS plasma model choices are most commonly the fluid approach for electrons including analytical Maxwell-Boltzmann distribution, and for ions Particle-In-Cell or backtracking method. When using Maxwell-Boltzmann electrons, it is recommended to use the non-linear Poisson solver since this is more robust for meshes which are larger than the Debye length (which is usually the case in LEO satellite models). For scientific satellites, it is possible to use kappa distributions and user-defined distributions to describe the plasma energy spectrum.

Figure 4-13 indicates how to set the ECSS-E-ST-10-04 worst case environment for GEO satellites.

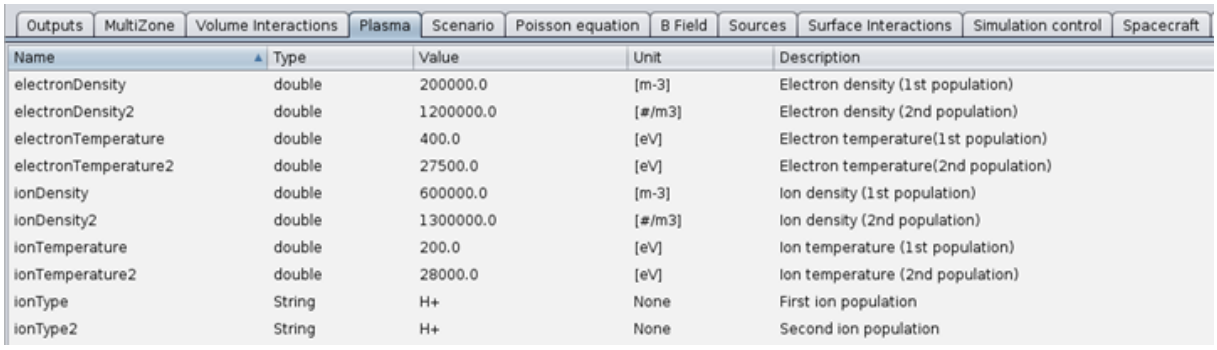

Name	Type	Value	Unit	Description
electronDensity	double	200000.0	[m-3]	Electron density (1st population)
electronDensity2	double	1200000.0	[#/m3]	Electron density (2nd population)
electronTemperature	double	400.0	[eV]	Electron temperature(1st population)
electronTemperature2	double	27500.0	[eV]	Electron temperature(2nd population)
ionDensity	double	600000.0	[m-3]	Ion density (1st population)
ionDensity2	double	1300000.0	[#/m3]	Ion density (2nd population)
ionTemperature	double	200.0	[eV]	Ion temperature (1st population)
ionTemperature2	double	28000.0	[eV]	Ion temperature (2nd population)
ionType	String	H+	None	First ion population
ionType2	String	H+	None	Second ion population

Figure 4-13: SPIS plasma parameters settings for the ECSS-E-ST-10-04 GEO worst case environment for surface charging.

4.5.8 Global parameters

4.5.8.1 GEO orbits

A default set of global parameters for a worst case GEO charging simulation can be selected within SPIS. Electrons are simulated as Maxwell-Boltzmann while ions are simulation by back-tracking. Usually the simulation is run until equilibrium and so a non-physical spacecraft capacitance is often used to allow a faster simulation convergence. However, for exit from eclipse simulations, a realistic capacitance is required.

4.5.8.2 LEO polar orbits

For the correct analysis of LEO orbits some additional effects are taken into account. The satellite is supersonic with respect to the thermal velocity of the low energy ions contained in the plasma environment. In order to be able to correctly take into account the ram and wake effects connected eminent in this situation it is important to model the low energy ions using the PIC model. The electrons are typically modelled using the Maxwell-Boltzmann fluid model which is needed in order to limit the total simulation time and memory demands. The overall Debye length in LEO orbits, even in the polar orbits with reduced thermal plasma density, is rather small. So, for a typical model it is not possible to mesh the satellite and especially the volume with a resolution smaller than the Debye

length. In this situation it is beneficial to use the non-linear Poisson solver implemented in the software. Since the worst case charging environments in LEO polar orbits is characterized by time limited auroral arcs the potentials on the satellite do not reach a steady state in this timeframe. So, it is of high importance that realistic estimations of the satellite capacitance towards the plasma are used so that the correct time progression of the potentials is simulated in the software.

4.5.8.3 Time-dependent potential variation

The time to reach equilibrium satellite potentials depends on the plasma environment and on the satellite geometry and covering materials. The absolute spacecraft potential usually changes within the time scale of a few millisecond due to the small spacecraft capacitance with respect to the environment. In the thick sheath limit, the capacitance of a sphere in vacuum can be used to set the spacecraft capacitance Csat. In GEO, Csat is about 1 nF. In the thin sheath limit which can be encountered in LEO, Csat can be approached by a capacitor of thickness the Debye length.

When the satellite is covered by large areas of dielectric, the transient phase can be totally controlled by the time for them to charge. As they are generally thin with respect to the Debye length, they need a much larger amount of time to charge. As a consequence both differential and absolute charging can reach equilibrium within tens or hundreds of seconds typically.

For PEO worst case charging estimations, the satellite is charged by the auroral electrons lasting on the order of up to ten seconds which is generally insufficient for the spacecraft to reach equilibrium. During GEO and MEO worst case environments for surface charging, hundreds of volts of differential potential can also occur before reaching the equilibrium.

ESD triggering can occur, which in turn discharges the spacecraft capacitance or some differential potential on the spacecraft.

Time-dependent changes in the environment can cause potential variations. In particular, the exit from eclipse falls into this category. In SPIS, this situation is modelled using the "EclipseExit" scenario defining the variation of sunlight flux with time. In the default ExclipseExit scenario, the satellite is in eclipse when a substorm representative of the ECSS-E-ST-10-04 starts at $t = 0$ s. At $t = 1000$ s the satellite starts exiting the shadow of the Earth. Generally, this produces a sudden decrease in the absolute spacecraft potential (due to small Csat) while the differential voltage of dielectrics remains relatively unchanged (due to large dielectric capacitances). The probability of ESD triggering on solar panels is can then be high. Secondary arcing is a concern since the solar arrays power progressively increase when exiting the eclipse.

Other transient situations such as changes in the plasma and sun orientation or turn on/off of electrical thrusters can also cause significant changes to the potential distribution of the spacecraft.

4.5.9 Consistency checks

There are several basic consistency checks which can be performed after a simulation has been finished. Here is a non-exhaustive list of things which can be looked at to check the sanity of the simulation results:

- Check potential distribution in the volume and especially on the outer simulation boundary.
  - It is important to keep the potential distribution on the outer boundary smooth and ideally to keep the potential there much lower than the spacecraft potential.
- Compare the calculated results versus the plasma properties which have been set in the simulation.

  - The negative charging in principle is expected not to exceed roughly three times the electron temperature in eV.
  - No positive potentials above about 20 V are possible.
- For simulations where the equilibrium state is reached the charging on different surfaces can be compared to values which are expected based on the conductivity and SEE values for the corresponding surfaces.
  - Surfaces with materials with lower conductivity in principle charge more negative than other surfaces if the SEE properties are comparable.
  - For surfaces with comparable conductivity and thickness the one with the lower overall SEE is expected to be more negative than the one with higher SEE.
- Check the potential on the outer boundary of the simulation volume; are there any strange potentials visible since usually the potential in the volume relaxes down to 0 V potential of undisturbed plasma.
- Check total current is null (or at least negligibly small compared to the initial current) at equilibrium and check net current on each node is consistent with conductivity.
- For GEO, have key parameters reached equilibrium? (For LEO there is possibly not enough time to reach equilibrium but it is important the capacitances are realistic).

5
Internal Charging

5.1 Fundamentals

5.1.1 Introduction

Internal charging in spacecraft occurs when particles have enough energy to penetrate beneath the spacecraft skin and become deposited inside materials or on internal structures. There is not always a clear distinction between surface and deep-dielectric charging because thick dielectrics on the spacecraft surface are subject to charge deposition over a range of depths and charge build-up near the surface and within the material both contribute to the electric fields within the structure. However, there are practical reasons for treating internal charging separately from surface charging:

Surface charging is associated with large currents of low to medium energy plasma (up to tens of keV) which causes both absolute and differential spacecraft charging on timescales of seconds to minutes. For internal charging, the currents of higher energy electrons (typically hundreds of keV and above) responsible for this effect, are much lower and generally vary over longer timescales. Unlike for surface charging, photoemission does not play a major role and ions are generally not significant. The time-scale for charging is often strongly influenced by the charging time-constant of the material. The most serious consequence of internal charging is electrostatic discharge (ESD). This can inject current directly into electrical circuits or indirectly generate currents via radiated electric fields.

5.1.2 Floating metals

Internal charging includes the charging of floating metals within a spacecraft. Here charging is very much like the surface charging of a floating metallic part on the spacecraft surface. These floating metals are often very thin and they are often capacitive-coupled to the underlying dielectric. Negative charging from penetrating electrons can lead to an inverted potential gradient where the metal is strongly negative with respect to surrounding structures and the resulting ESD can occur at potential differences of a few hundred volts and leads to the complete discharge of all the charge in the metal. Unlike for surface materials, these metals are not able to be discharged by sunlight-induced photoemission or by contact with plasma populations. Hence, if they are well insulated, these structures can build up a high potential over an extended time period, despite low charging currents.

5.1.3 Insulators

Internal charging in insulators (also called deep-dielectric charging) occurs because penetrating electrons remain embedded within insulating material. ESD can occur when the internal electric field exceeds the dielectric strength (typically ~10MV/m) of the material. Although insulators are employed because of their very low conductivity, this conductivity is not zero and leakage current can play a

significant moderating role for some materials. In particular, when radiation doses are high, radiation-induced conductivity can lead to a raised bulk conductivity and there can also be electric field induced conductivity at high electric fields.

5.1.4 Charge Deposition

Energetic electrons penetrate spacecraft surfaces and become deposited in internal materials. The depth of penetration depends on the electron energy and the material properties, especially its density. The 'Range' of an electron can be defined in different ways but it corresponds roughly to the maximum penetration depth at a particular energy. Due to scattering, most electrons are stopped at smaller depths than this as shown in Figure 5-1.

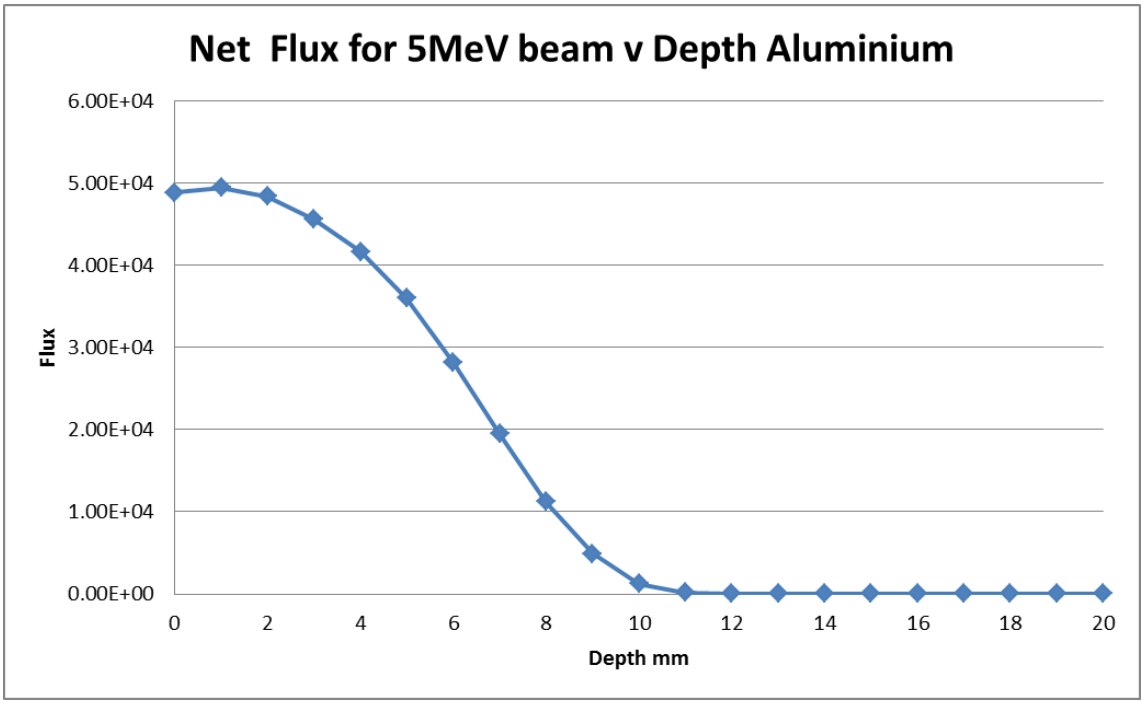

Figure 5-1: Mulassis [RD.10] simulation of net flux (forward minus backward travelling) due to a 5 MeV incident beam in a planar sample of Aluminium. CSDA range is approximately 11,4 mm

5.1.5 Conductivity

In dielectrics, electrons belonging to atoms are in energy states beneath the conduction band and have only an extremely small probability of spontaneously becoming an electron hole pair. This process is highly dependent on temperature and hence there is a strong positive correlation between temperature and conductivity for these materials. A formula describing the temperature dependence of conductivity was proposed by Adamec and Calderwood [RD.11], where:

$$\sigma(T) = \frac{\text{const.}}{kT} \exp\left(-\frac{E_A}{kT}\right)$$

Equation 9

where T is temperature and EA is the activation energy, a constant of the dielectric. The effect of electric field can be included using another formula based on work by Adamec and Calderwood [RD.11], i.e.

$$\sigma(E,T) = \sigma(T)\left(\frac{2+\cosh(\beta_F E^{1/2}/2kT)}{3}\right)\left(\frac{2kT}{eE\delta}\sinh\left(\frac{eE\delta}{2kT}\right)\right)$$

Equation10

where E is electric field, $\beta_F = \sqrt{\frac{e^3}{\pi\varepsilon}}$, δ is jump distance, e is the charge on an electron.

Radiation dose-rate induced conductivity is simply described in DICTAT [RD.12] and other tools by the empirical formula

$$\sigma(J) = K_p \dot{D}^{\Delta}$$

Equation11

where $\dot{D}$ is dose rate (rads s^{-1}) and Kp and Δ are measured constants of the material. This formula is too simplistic for some materials, like FEP Teflon, and Hanna et al 2014 [RD.13] have produced a more realistic algorithm. This explains the formation of both trapped and free charges within the material. Observed charging behaviour can be explained by the rate of production of these different types of charge and the probability of de-trapping and recombination.

$$\frac{dn}{dt} = g - \alpha n p_t - \frac{n}{\tau_n} + \frac{n_t}{\tau_{nt}}$$

$$\frac{dn_t}{dt} = \frac{n}{\tau_n} - \frac{n_t}{\tau_{nt}} - \alpha p n_t$$

$$\frac{dp}{dt} = g - \alpha n_t p - \frac{p}{\tau_p} + \frac{p_t}{n_{pt}}$$

$$\frac{dp_t}{dt} = \frac{p}{\tau_p} - \frac{p_t}{\tau_{pt}} - \alpha n p_t$$

Equation 12 from [RD.13]

Here g is the rate of formation of free electron-hole pairs, free electron and hole densities are n and p respectively, nt and pt are trapped electron and hole densities, α is a recombination coefficient and τn and τp are mean electron and hole lifetimes before becoming trapped and τnt and τpt are the mean lifetimes before trapped electrons and holes become un-trapped. Free electrons and holes provide the conductivity of the material.

$$\sigma_{RIC} = e(\mu_n n + \mu_p p)$$

Equation 13

Here σ is conductivity, μn and μp and electrons and hole mobilities. These equations show that, even under constant irradiation, the conductivity can rise over time as free electron-hole production initially outstrips recombination. Then this rise stops when recombination accelerates and it limits the free electron hole increase. As a result, FEP Teflon, under constant irradiation was seen in [RD.13] to show a rise, fall and rise again in surface potential.

5.1.6 Time-dependence

To a first approximation, many dielectrics can be simplified to be represented by a simple parallel plate capacitor. From a starting value of zero, the electric field *E* at time *t* is given by:

$$E = \frac{J}{\sigma}\left(1 - \exp\frac{-t}{\tau}\right)$$ Equation 14

Where *J* the current density and σ is total conductivity. This means the field exponentially approaches the equilibrium electric field. The time-constant τ depends on the total resistance *R* and capacitance *C*, summed across the structure, i.e.

$$\tau = RC = \sum \frac{\varepsilon}{\sigma}$$ Equation15

In practice, even for a simple dielectric, the conductivity can change during the irradiation due to the radiation and electric field effects already described and as a result the time-dependence can deviate from this exponential behaviour.

5.2 General methodology

5.2.1 Introduction

Since there are many aspects of the space environment that can have a detrimental effect on a spacecraft or its operations, it is part of the spacecraft design process to make an assessment of how severe the effects can possibly be. These analyses require an understanding of the environment and can involve testing in the laboratory, computer simulation or both. Where space systems are re-used in the same or a similar environment, heritage can also play an important role.

Internal charging effects are similar to external charging effects except that the dielectric breakdown occurs inside the spacecraft outer surface. In general, the discharge site of internal charging induced ESDs can be located much closer to sensitive electronics devices and circuits. One possible discharge location can be an external harness insulation which let ESD transients propagate into sensitive on-board electronics circuitry. For this reason often internal charging effects impose a much higher threat to the actual spacecraft design. In order to distinguish the internal charging induced ESDs from the general term “ESD”, the internal charging induced electrostatic discharges are often called “internal ESDs” or “IESDs”.

Internal charging is dependent on the spacecraft geometry as well as on the actual in-orbit electron environment which the spacecraft traverses during the course of its mission life. The spacecraft geometry determines the level of shielding available (leading to a reduction of charge deposition on critical dielectrics and isolated metals). The actual charge deposition and distribution depends critically on the grounding and the actual 3D geometry of the materials involved. The high energy electron environment, usually from the trapped radiation belt population, determines the amount of charge impinging on the spacecraft and therefore the potential to develop high levels of internal charging.

For internal charging, the complete spacecraft geometry is of less importance to a particular piece of equipment than its local shielding and internal construction. Unfortunately, realistic laboratory testing is difficult because it is hard to reproduce the severe radiation environment and to test over the long time-scales associated with internal charging. Hence computer simulation is an essential part of the analysis.

In this Section we discuss the general requirements and methods of internal charging analyses.

5.2.2 Internal charging analyses

The way to decide on the need to perform an internal charging analysis for a particular piece of equipment is illustrated in Figure 5-2

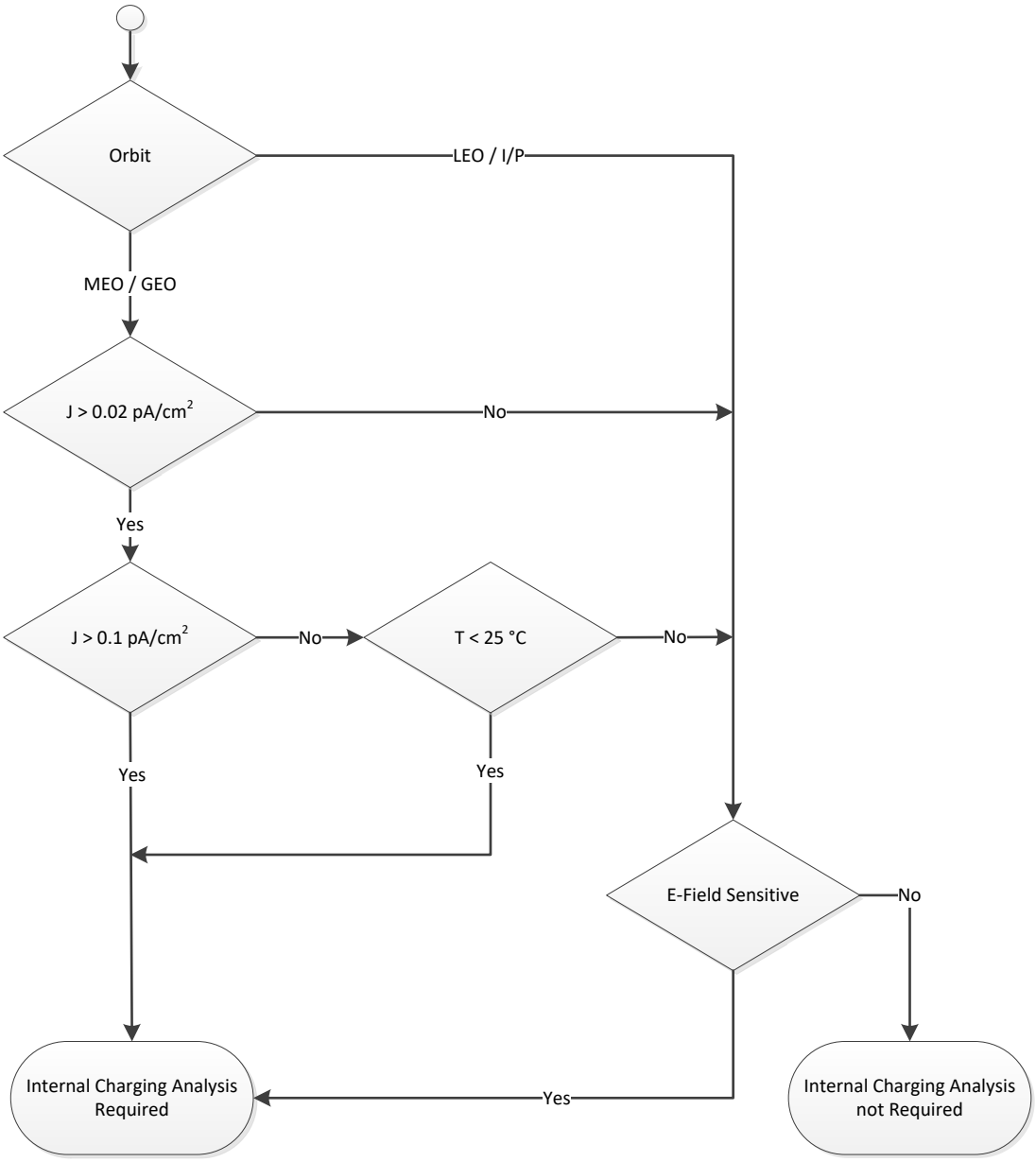

Figure 5-2: Decision flow diagram for performing an internal charging analysis

Orbit is generally the first consideration and the charging engineer identifies the plasma environment within which the satellite is exposed during its mission, starting from the launcher separation and ending with the disposal phase. If the spacecraft remains in LEO or goes directly into in interplanetary space it is not subject to charging fluxes sufficient to lead to ESD.

In order to limit the internal charging analysis to the critical components and pieces of equipment, a "safe-level" threshold current is has been calculated, defining the current density level below which no further internal charging related analysis is required. ECSS-E-ST-20-06 defines the "safe-level" in terms of incident electron current. With the use of common radiation transport tools the corresponding shielding level is calculated, e.g. to define the corresponding "charging current-depth curve", defining the electron current levels as a function of the shielding aluminium-equivalent thickness, which constitutes the local internal charging environment.

Some specialised components, which are directly sensitive to electric fields, also need to be subject to an internal charging analysis, even below the current threshold. However, these are rare.

For all elements identified as critical in terms of internal charging effects, the corresponding geometry model and the relevant material characteristics need to be defined. When no adequate material parameters can be identified because of lack of test data available, a dedicated test program is considered. The quality of the internal charging analysis depends very much on the quality of the material characterization.

In general it is considered valuable to perform 1D internal charging analysis where sufficient, and to perform more detailed 3D analysis when the 1D internal charging analysis results are not sufficient to demonstrate that no internal charging induced ESDs take place, or when the equipment in question cannot be simplified by a 1D geometry (for example wire harness and connectors).

In case it is needed, design mitigation measures are considered to either reduce the probability of internal charging induced ESDs or to reduce the severity of the effect below the acceptable limits of the space program.

If the presence of an ESD cannot be excluded, it is recommended to perform calculations and/or simulations of the expected ESD characteristics, in order to assess the impacts of the ESD.

5.2.3 Critical aspects with respect to worst case internal charging analysis

Here we identify a process to investigate the vulnerability of dielectric materials:

a. Make an inventory of the structures that can become charged

   1. Dielectrics with floating metalisation: i.e. spot shielding, board metallisation
   2. Dielectrics with low conductivity. Extract from the DML (Declared Material List) all dielectric according to a low conductivity criterion

      NOTE If conductivity is implemented in the DML, this can be an automatic process

   3. Dielectrics that are thick with respect to their shielding
   4. Space exposed dielectrics: All those which can store charge in their depth
   5. Dielectrics inside the spacecraft: All those whose thickness is higher than the lowest shielding thickness of the surrounding spacecraft body

NOTE Be careful, in case of wiring paths through holes only covered by MLI and/or Chofoil™. Here the thickness to take into account can be around 100 μm Al equivalent

6. Dielectrics internal to electronic boxes: All those which thickness is above the total surrounding thickness including box and spacecraft walls

NOTE If the 3D-Radiation analysis is missing, the thickness to be considered is the sum of the lower thickness of box and spacecraft walls. Typically value is around 3mm

Thick dielectrics often include mirrors, lenses, optical filters, dielectric stiffeners (PEEK, epoxy) and thick printed circuit boards.

b. Consider the radiation flux

The flux to consider is the part of the positive or negative particle spectrum that passes through the surrounding shielding and is stored in the dielectric. In a first approximation, this can be estimated for each material from the charging current-depth curve. The energy start point is defined by the surrounding shielding and the energy bandwidth is defined by the thickness of the dielectric. An example of a current-depth curve is shown in Figure 5-3 and Table 5-1. It shows orbit-averaged current density for a geostationary orbit for the worst part of the solar cycle, the worst season in the year and the worst longitude.

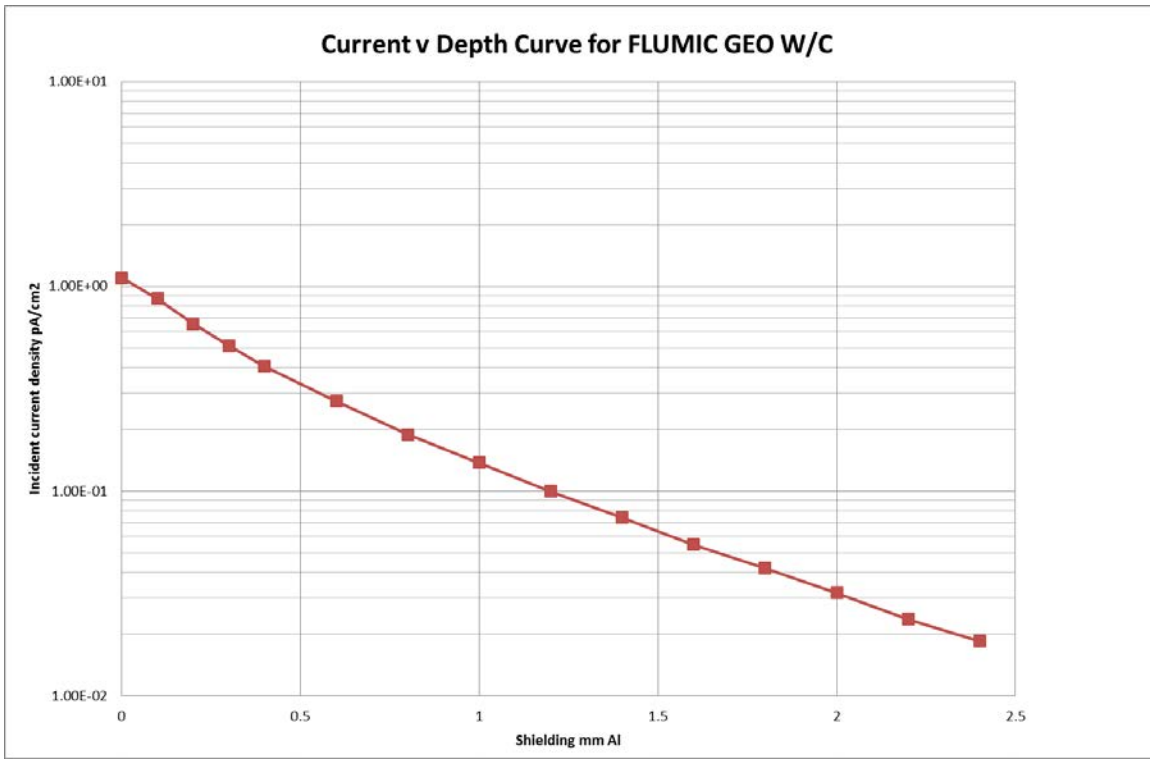

Figure 5-3: Current density v shielding depth curve for a geostationary orbit with longitude 195deg East with nominal date 21/09/1994 according to the FLUMIC model as calculated by the Mulassis tool in SPENVIS. The FLUMIC spectrum was calculated by DICTAT in SPENVIS.

Table 5-1: Current density v shielding depth values for a geostationary orbit with longitude 195deg East with nominal date 21/09/1994 according to the FLUMIC model as calculated by the Mulassis tool in SPENVIS. The FLUMIC spectrum was calculated by DICTAT in SPENVIS.

Energy (MeV)	Current density (pA/cm^2)
0	1,10E+00
0,1	8,70E-01
0,2	6,56E-01
0.3	5,12E-01
0,4	4,07E-01
0,6	2,76E-01
0,8	1,89E-01
1	1,37E-01
1,2	9,99E-02
1,4	7,41E-02
1,6	5,48E-02
1,8	4,20E-02
2	3,19E-02
2,2	2,37E-02
2,4	1,85E-02

A worst case for any Earth orbit can be obtained by looking at the current density versus depth for the most intense part of the radiation belt as shown in Figure 5-4 and Table 5-2. This corresponds to L=4,4 at the magnetic equator, and has the same temporal variation in the FLUMIC model.

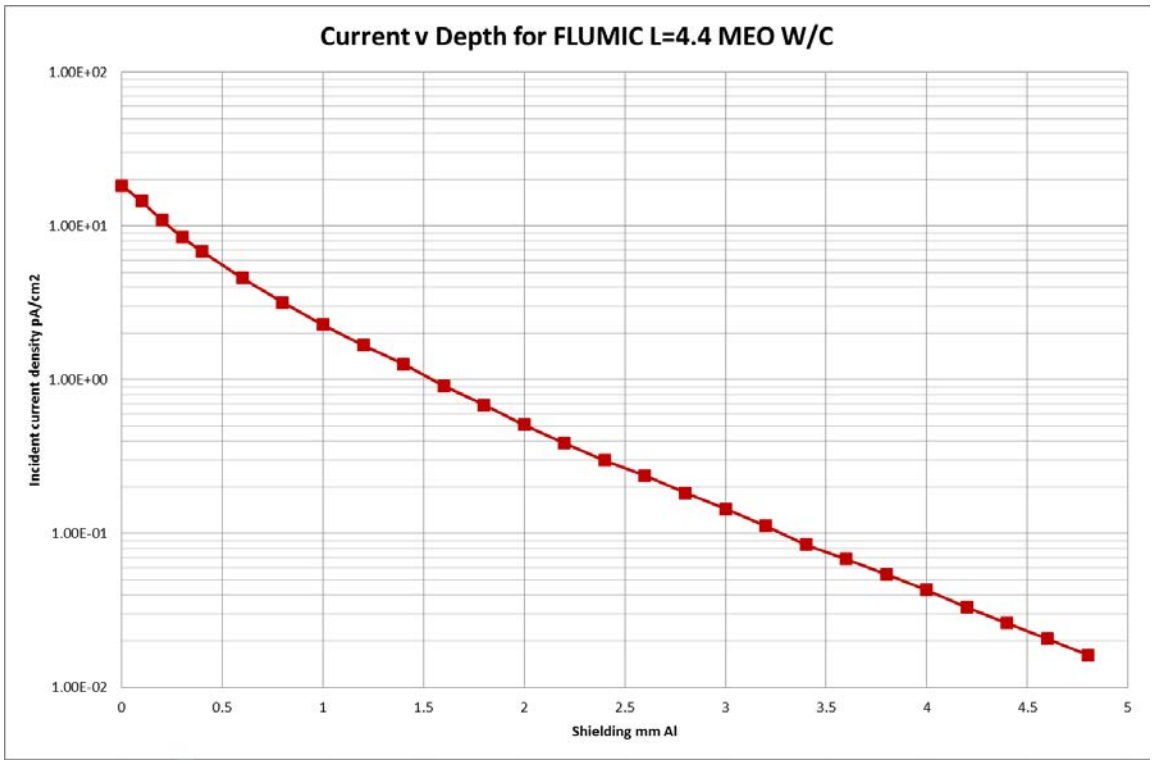

Figure 5-4: Current density v shielding depth curve for the peak of the outer radiation belt L=4,4, B/B0=1,0 with nominal date 21/09/1994 according to the FLUMIC model as calculated by the Mulassis tool in SPENVIS. The FLUMIC spectrum was calculated by DICTAT in SPENVIS.

Table 5-2: Current density v shielding depth values for the peak of the outer radiation belt L=4,4, B/B0=1,0 with nominal date 21/09/1994 according to the FLUMIC model as calculated by the Mulassis tool in SPENVIS. The FLUMIC spectrum was calculated by DICTAT in SPENVIS.

Energy (MeV)	Current density (pA/cm²)
0	1,83E+01
0,1	1,45E+01
0,2	1,09E+01
0,3	8,45E+00
0,4	6,81E+00
0,6	4,59E+00
0,8	3,19E+00
1	2,28E+00
1,2	1,68E+00
1,4	1,26E+00

Energy (MeV)	Current density (pA/cm²)
1,6	9,09E-01
1,8	6,87E-01
2	5,09E-01
2,2	3,88E-01
2,4	2,99E-01
2,6	2,37E-01
2,8	1,83E-01
3	1,45E-01
3,2	1,12E-01
3,4	8,45E-02
3,6	6,83E-02
3,8	5,43E-02
4	4,31E-02
4,2	3,32E-02
4,4	2,62E-02
4,6	2,07E-02
4,8	1,62E-02

After this first assessment, dangerous or borderline situations requires further analysis.

c. Perform analysis

It is important to compute potential dangerous situations with a realistic 3D analysis tool or 1D modelling if no 3D tool is available. For a good accuracy the RIC radiation induced conductivity needs to be considered in the analysis. Otherwise, results can be overestimated.

It is important that the analysis includes, current deposition, the conductivity of each dielectric and its variation due to instantaneous dose, total dose, temperature and thermal cycling and UV light.

d. Perform testing

It is important that testing aims to deliver a realistic worst case charging current along with a realistic dose-rate at the lowest expected temperature.

It is important if possible, that testing considers material properties at BOL, MOL, EOL and specific situations like eclipse outcome for space exposed dielectric for example.

5.2.4 Modelling aspects for internal charging analyses

5.2.4.1 Choosing where simulation is necessary

Unlike surface charging, internal charging is a local effect and simulations are made at the level of individual dielectric structures. In 3D simulations, the whole of the spacecraft can be simulated for the particle transport but only the local structure needs to be simulated regarding the deposited charge, conduction and resulting electric fields and voltages.

Since internal charging potentially concerns the dielectric structures throughout the spacecraft from the surface to structures deep inside the spacecraft, it is necessary to be selective about where a detailed analysis is required. The following structures are identified as requiring further analysis:

- Where the dielectric is thicker than the surrounding aluminium-equivalent shielding.
- Where the shielding is thinner than critical thickness levels defined by ECSS-E-ST-20-06 in requirement 9.3.f.
- Where the current is above the current threshold defined in ECSS-E-ST-20-06 requirement 9.3.f.

5.2.5 Environment

The external environment of interest for internal charging effects is predicted by dedicated environment models specialized for the purpose of internal charging effects, such as FLUMIC [RD.12], MOBE-DIC [RD.16], and AE9/SPM [RD.17]. The local charging environment is determined by the modulation by available shielding.

Other radiation environment models which predict the electron flux at a given orbit do not usually provide a realistic worst case environment due to the different time-scales considered (years instead of e.g. days for the internal charging process). Especially the outer electron belt is known to be highly dynamic, which is averaged-out in the long-term radiation models.

5.2.6 Geometry

Depending on the software analysis tool used, the geometry model is defined using a 1D or 3D approximation. The specifics of 1D vs 3D modelling are discussed in the following Sections.

5.2.6.1 1D Modelling

For simple structures (e.g. planar dielectrics on a metallic conductor) a 1D analysis is enough. It is important to know the conductivity of the material. The worst case current deposited in the dielectric can be calculated from a variety of ways (e.g. Monte Carlo transport code or analytical equations). Dedicated 1D internal charging codes can be useful here, e.g. DICTAT [RD.12], NUMIT [RD.14] or MCICT [RD.15].

As an initial step, Ohm's Law can be used to estimate the maximum electric field using the bulk conductivity at the lowest temperature and ignoring radiation induced conductivity. Where the bulk conductivity is high, this can exclude some dielectric structures from further analysis.

Where further analysis is needed, the 1D internal charging codes consider radiation induced conductivity and electric field induced conductivity but these require further material parameters

The DICTAT tool is a 1D internal simulation code that is available in SPENVIS or stand-alone. 1D models are constructed using a planar or cylindrical geometry structure. The code calculates the electric field and potential of the dielectric material under analysis based on the environment as modified by shielding. In case multiple dielectric materials exist (separated by a conductive element), then a separate geometry model is created for the different dielectrics. For cylindrical geometry models, typical parameters include the core conductor radius, shielding thickness, the thickness of the dielectric material, parameters of the dielectric material under analysis (refer to Section 5.2.7), and the grounding (inner surface, outer surface, both surfaces). Planar geometry models are defined by the thickness of the dielectric material, the parameters of the dielectric material under analysis, and the grounding path (inner surface, outer surface, both surfaces).

MCICT is also 1D. It uses Monte Carlo radiation transport calculations based on Geant-4 to calculate the deposited current and dose rate. This can be more accurate than the equivalent DICTAT calculations but is computationally more expensive. Only planar geometries are simulated but multiple dielectric and conductor layers are possible. For conducted current and conductivity, it uses models very similar to DICTAT.

5.2.6.2 3D modelling

3D internal charging models are more complex than simple 1D models, involving various geometrical structures defining a small part under analysis, or the model of a specific equipment under analysis or a complete spacecraft. 3D models are used when simple 1D models are too different from the actual geometry of the structure or do not provide sufficient margin to the electric field breakdown threshold of the material under analysis.

The deposited current is calculated and, depending on the tool used, the radiation-induced conductivity as well as the 3D distribution of electric fields and current paths.

In order to identify if the electric field breakdown threshold of the material under analysis is exceeded, the deposited current is translated into the electric field generated across the dielectric element under analysis.

5.2.7 Materials parameters

It is important to adequately select suitable material parameters in order to achieve a realistic worst case internal charging analysis.

Relevant materials parameters include:

- Dielectric constant (ε)
- Dielectric thickness (d)
- Temperature of the dielectric material under analysis (T)
- Conductivity (σ)
- Electric field breakdown threshold (E_{crit})
- RIC dose rate factor (k_p)
- Activation energy (E_A)

If a more sophisticated radiation-induced conductivity model (like the model of [RD.13] described in section 5.1.5) is used then further parameters to characterize this aspect of the material can be required.

It is important to perform an analysis on the possible evolution of material properties with time spent in orbit. Three typical cases can be considered as of particular interest: BOL, MOL and EOL.

5.2.8 Simulation tools in 1D and 3D

The 1D code DICTAT can be run online from the SPENVIS web site: https://www.spenvis.oma.be. Alternatively there is a stand-alone version of the Fortran code. Simulations in planar and cylindrical geometry are possible. This code uses a simple analytical approximation for particle transport and for dose rate.

The 1D code MCICT, developed by RadMod Research Ltd. For ESA, is seen as the successor to DICTAT. It can be run in planar mode and particle transport and dose calculations are based on the

Geant-4 Monte Carlo code, which offers better accuracy. At the time of writing this handbook, it is being integrated into the SPENVIS framework and in future be available online. In the meantime a stand-alone version is available, with permission, from ESA.

For 3D simulations, the CIRSOS code has been developed by a consortium composed of RadMod Research, Artenum, Astrium, Etamax DHC, INTA, Kallisto Consulting, PSI and ONERA for ESA. It combines Geant-4 with an internal charging version of SPIS, SPIS-IC. Geant-4 is used for particle transport while SPIS is used for the 3D electric field calculation. The CIRSOS code provides an interoperability bridge to facilitate exchanges geometrical models between radiation dose calculations and internal charging. CIRSOS is available with Europe via ESA. A version of SPIC-IC for internal charging calculations without this collaborative aspect is also available from the SPINE community http://dev.spis.org/projects/spine/home/spisic. The SPIS-Services edition of SPIS-IC, available via Artenum and ONERA, includes interoperability functions with the GRAS radiation tool developed by ESA based on Geant 4, through the MoORa application. It also integrates the Extended GDML editor (EDGE), a wysiwyg CAD tool dedicated to GDML format used by Geant4-based models.

5.2.9 Scenarios

Internal charging analyses are usually carried out considering worst case electron charging environments and assuming a relevant duration. However, time series of spectra can be more realistic when the environment is varying over time-scales that are shorter than or similar to the characteristic charging and discharging timescale of materials. Both DICTAT and MCICT allow a time-series of spectra, e.g. arising from an orbital calculation, to be input. The time constant of a material is influenced by the temperature and radiation induced conductivity as well as material bulk conductivity. Materials that experience low dose rate and are cold can have very long time constants.

5.2.10 Important Outputs

Important outputs of the internal charging analysis include the assessment of the maximum electric field generated within the dielectric material under analysis and the differential voltage to surrounding elements, including that of floating metalisation. It is important to compare these parameters to the critical values specified in ECSS-E-ST-20-06.

6
General aspects of surface and internal charging analysis

6.1 Material characterization aspects

The material specification is very important aspect of the charging assessment and strongly affects the results of the simulations. Hence the user needs to take care to choose the best material characteristics from the available databases or to perform the needed characterization for missing material parameters. Material parameters can change as a result of aging, radiation, temperature changes, sputtering, contamination and outgassing. It is important that the characterization tests take these into account as far as possible.

6.2 Charging analyses and project phases

6.2.1 Phase 0: Mission analysis

First estimate of highest level of charging is performed. This can be based on past experience and approximate orbit type. Details of plasma regions encountered by different orbit types are provided in Annex A.

6.2.2 Phase A: Feasibility

Detailed environment specification is produced including as a minimum mean values and worst case scenarios.

Order of magnitude estimates of charging level and ground potential can be performed based on these environment specifications and planned spacecraft configuration.

Specific material or charge mitigation requirements to ensure mission objectives are investigated.

Environment specifications are provided at System Requirement Review together with specific requirements for addressing charging issues.

6.2.3 Phase B: Preliminary definition

All problems area related to charging are identified. This in general includes configurations with possible risk of electrostatic discharge such as triple points (interface of metal, plasma and dielectric) but also all possible other risks. Scientific missions with plasma measurements can have charging concerns with different threshold level than for ESD. Such problems area need also to be identified.

This preferably is based on a 3D model of the spacecraft with representative distribution of conductive and non-conductive surface including thermal blankets and solar arrays. Spatial resolution of 10 cm is usually enough.

The charging analysis report is provided at the Preliminary Design Review as part of the Design Justification file.

6.2.4 Phase C: Detailed definition

Each identified problem area (i.e. where there is a significant risk of exceeding a critical voltage threshold) is subject to a convincing detailed analysis. Although it is usually enough to derive an order of magnitude of the effect this can still require detailed spatial resolution. Therefore, for computational reasons it can rely on a range of simplifying hypotheses and on a detailed modelling of only part of the system but consistent with the global behavior of the full system.

It is important to consider an experimental set-up whenever possible to verify the predicted level of charging of sensitive elements.

Demonstration of charging behaviour of critical elements at Critical Design Review.

Description of the tests to be performed for the qualification.

6.2.5 Phase D: Production

Verification of immunity against ESD and other electrostatic issues by models and tests.

6.2.6 Phase E: Utilisation

Modelling of effects in orbit.

Annex A
Orbit plasma environment

A.1 Plasma environment for different Earth orbits

This Annex presents an overview of the different plasma environment encountered on different terrestrial orbits.

Table A-1: Type of environments and order of magnitudes of density and temperature encountered along typical orbits

	Ionosphere $n \sim 10^{9} - 10^{11}\ m^{-3}$ T ~0,1eV	**Plasma-sphere** $n \sim 10^{6} - 10^{9}\ m^{-3}$ T ~1eV	**Auroral arcs** $n \sim 10^{6}\ m^{-3}$ T ~1-10 keV	**Plasmasheet** $n \sim 10^{6}\ m^{-3}$ T ~1–10 keV	**Lobe** $n \sim 10^{5}\ m^{-3}$ T ~1 eV	**Magneto-sheath** $n \sim 10^{6}\ m^{-3}$ T ~100 eV	**Solar wind** $\sim 10^{7}\ m^{-3}$ T ~1 eV	**Induced plasma** $n \sim 10^{6} - 10^{14}\ m^{-3}$ T ~1 eV
LEO (<40 deg)	X	X						X
LEO (>40 deg)	X	X	X	X	X			X
GTO/HEO	X	X		X	X	X	X	X
GEO/MEO		X		X	X	X	X	X
L1, L4, L5							X	X
L2				X	X	X	X	X

Table A-2: Order of magnitudes of key plasma and charging parameters expected in typical environments

Environment	**Density (SI)**	**Spacecraft relative drift velocity (SI)**	**Temperature (eV)**	**Debye length (SI)**	**Electron current density (SI)**	**Potential of non-sunlit surface (V)**	**Spacecraft Floating potential (V)**
Ionosphere (min)	1,E+09	7,E+03	1,E-01	7,E-02	-2,E-05	-0,1	-0,1 to -1
Ionosphere (max)	1,E+12	7,E+03	1,E-01	2,E-03	-2,E-02	-0,1	-0,1 to -1
Plasmas-phere	1,E+07	7,E+03	1,E+00	2,E+00	-5,E-07	-1	-10 to +10
Auroral arcs	1,E+06		1,E+04	7,E+02	-5,E-06	-1,E3	+10 to -1,E3
Plasma-sheet	1,E+06	7,E+03	1,E+04	7,E+02	-5,E-06	-1,E3	+10 to -1,E3
Lobe	1,E+05		1,E+02	2,E+02	-5,E-08	-1,E2	+10
Magneto-sheath	1,E+06		1,E+02	7,E+01	-5,E-07	-1,E2	+1
Solar wind	1,E+06	3,E+05	1,E+00	7,E+00	-5,E-08	-1	+1
Photo-emission	1,E+09		1,E+00	2,E-01	5,E-05	n/a	n/a

A.2 GEO worst case environments

A.2.1 Introduction

The literature provides a list of severe environments to be considered as an envelope of worst case environments for surface charging. Some of the most important are described in this section.

A.2.2 ECSS

"Space engineering – Space Environment," ECSS-E-ST-10-04, provide a worst-case environment for surface charging at GEO defined as the sum of two Maxwellian energy distributions for both electrons and protons.

Table A-3: ECSS-E-ST-10-04 worst case charging environment

Population	Electron density (cm^{-3})	Electron temperature (keV)	Ion density (cm^{-3})	Ion temperature (keV)
Population 1	0,2	0,4	0,6	0,2
Population 2	1,2	27,5	1,3	28,0

A.2.3 NASA

NASA-TP-2361:1984 [RD.34] and NASA-HDBK-4002A:2011 [RD.22]recommend using the single Maxwellian distributions given in Table A-4 and to use more realistic plasma representations if the worst-case analysis shows a possible ESD problem, i.e. differential potentials voltage larger than 100 Volts. More realistic plasma conditions are given in Table A-5 (Table 16 from NASA-HDBK-4002A).

Table A-4: NASA-HDBK-4002A worst case charging environment

Electron density (cm^{-3})	Electron temperature (keV)	Ion density (cm^{-3})	Ion temperature (keV)
1,12	$1{,}2\times10^{4}$	0,236	$2{,}95\times10^{4}$

Table A-5: NASA 'more realistic' geosynchronous worst case environment specification

NASA-HDBK-4002A

Table 16—Worst-Case Geosynchronous Environments

ELECTRONS	Deutsch* ATS-6	Mullen** SCATHA	Mullen*** SCATHA
Number density (ND) (cm^{-3})	1.22	0.9	3
Current density (J) (nA cm^{-2})	0.41	0.187	0.501
Energy density (ED) (eV cm^{-3})	2.93E+04	9.60E+03	2.40E+04
Energy flux (EF) (eV cm^{-2} s^{-1} sr^{-1})	2.64E+13	6.68E+12	1.51E+13
Number density for population 1, N1, cm^{-3}	0	--	--
Parallel	--	0.2	1.0
Perpendicular	--	0.2	0.8
Temperature for population 1(T1) (keV)	0	--	--
Parallel	--	0.4	0.6
Perpendicular	--	0.4	0.6
Number density for population 2 (N2) (cm^{-3})	1.22	--	--
Parallel	--	0.6	1.4
Perpendicular	--	2.3	1.9
Temperature for population 2 (T2) (keV)	16.0	--	--
Parallel	--	24.0	25.1
Perpendicular	--	24.8	26.1
Electron average temperature (Tav) (keV)	16	7.7	5.33
Electron root-mean-square temperature (Trms) (keV)	16.1	9	7.33
IONS (PROTONS)	**Deutsch* ATS-6**	**Mullen** SCATHA**	**Mullen*** SCATHA**
Number density (ND) (cm^{-3})	0.245	2.3	3
Current density (J) (nA cm^{-2})	0.00252	0.00795	0.0159
Energy density (ED) (eV cm^{-3})	1.04E+04	1.90E+04	3.70E+04
Energy flux (EF) (eV cm^{-2} s^{-1} sr^{-1})	2.98E+11	3.42E+11	7.48E+11
Number density for population 1, N1, cm-3	0.00882	--	--
Parallel	--	1.6	1.1
Perpendicular	--	1.1	0.9
Temperature for population 1, T1, keV	0.111	--	--
Parallel	--	0.3	0.4
Perpendicular	--	0.3	0.3
Number density for population 2, N2, cm-3	0.236	--	--
Parallel	--	0.6	1.7
Perpendicular	--	1.3	1.6
Temperature for population 2, T2, keV	29.5	--	--
Parallel	--	26	24.7
Perpendicular	--	28.2	25.6
Ion average temperature (Tav) (keV)	28.4	5.5	8.22
Ion root-mean-square temperature (Trms) (keV)	29.5	12	11.8

Note: Tav, Trms, and the ATS-6 two-Maxwellian parameters are averaged over all angles. The SCATHA two-Maxwellian parameters are for fluxes parallel and perpendicular to the magnetic field.
*Deutsch, 1982 ** Mullen and others (1981) *** Mullen, Gussenhoven, and Garrett, 1981

A.2.4 ONERA/CNES

Worst-case environments from GEO LANL spacecraft data between 1989 and 2005 are given in [RD.21]. It consists of triple Maxwellian distributions for electrons and protons representing the average environment fluxes over 86 seconds and over 15 minutes. The first environment is associated with the highest Flux of electrons at Energies above 10 keV (FE10k). The second environment concerns the Highest Flux of electrons at All Energies (HFAE). The third environment concerns high electron fluxes at low energies together with a Low electron Flux at High Energy (LFHE). Finally, the average environment during the longest events with a Potential Greater than 5 kV - in absolute - (PG5k) was also provided.

An additional triple Maxwellian distribution has been proposed in [RD.21] to fit the event measured by SCATHA on April 24th, 1979 at 0650 UTC, when the SCATHA potential reached -370 V when it was in sunlight, just before it reached -8 kV entering the Earth's shadow. The double Maxwellian fit of this event that was provided by Gussenhoven and Mullen,1983 [RD.20] is the current ECSS worst-case mentioned in Section A.2.1. The additional triple Maxwellian distribution presented in Table A-6 is based on the electron flux perpendicular to the magnetic field line presented in figure 6 of [RD.20]. It is referred as "3Maxwell Scatha 1979/4/24". It better represents the actual ~10 keV and >20 keV electron fluxes than single or double Maxwellian available in the literature.

According to [RD.19] the average proton distribution can be used to assess worst case charging environments.

Table A-6: Severe charging environments in GEO [RD.35]

Triple Maxwellian Distribution Parameters Used to Fit the LANL Worst-Case Environments and the SCATHA Event Measured on 24 April 1979

	FE10k-15 min	FE10k-86 sec	HFAE-15 min	HFAE-86 sec	LFHE-15 min	LFHE-86 sec	PG5k	3 M Scatha 1979/4/24
Electron Density (cm^{-3})								
N1	0.5	1	0.05	0.1	0.25	0.7	0.4	0.2
N2	0.6	1.5	0.2	0.3	1	1	0.1	2
N3	0.2	0.25	0.25	0.4	0.05	0.001	0.004	0.01
Temperature (keV)								
T1	1	0.5	0.5	1	0.5	1	5	0.1
T2	6	5	5	5	5	7	10	10
T3	15	15	20	20	10	20	30	50
Proton Density (cm^{-3})								
N1	0.1	1.0	0.2	0.05	0.2	0.15	0.03	1
N2	1	2.0	0.35	0.4	1.1	1.5	0.5	1
N3	0.01	0.3	0.15	0.5	0.007	0.004	0.005	0.05
Temperature (keV)								
T1	0.7	2	2	0.5	1	1	2	3
T2	15	20	15	5	15	15	12	20
T3	40	60	40	40	40	50	40	40

A.3 LEO/Polar

ECSS-E-ST-10-04 [RD.2] specifies a severe auroral charging environment based on an extreme DMSP charging event

— For E ≤17,44 keV:

$f(v) = 3{,}9 \times 10^{-18}\ \ s^3m^{-6}$	Equation A-1

— For E > 17,44:

$$f(v) = \frac{[N_0(m_e)^{3/2} \exp\{-(E-E_0)/kT_0\}]}{(2\pi kT_0)^{3/2}}$$	Equation A-2

Where:

f(v) is the distribution function in $sec^3\ m^{-6}$

N_0 is the density in m^{-3}

m_e is the electron mass in kg

kT_0 is the thermal energy in J

E_0 is in J

E is energy in J and parameters of the worst case environment are:

N_0 = 1,13E6 m^{-3}

kT_0 = 3,96 keV

E_0 = 17,44 keV

In practice, it is easier to use Maxwellian distributions in some charging simulation tools because this allows faster analytical calculations on currents. Hence, a Maxwellian fit to the above auroral distribution function, i.e. Temperature = 11 keV and density= 1,1E7 m^{-3} as proposed by Imhof et al 2016 [RD.8].

Note that due to the dynamic behaviour of this auroral environment is expected be a worst case for only up to 10 s, even though an auroral crossing can be up to 2 minutes.

For worst case auroral charging assessments, a thermal ion density of 125 cm^{-3} and temperature 0,2 eV is specified.